HAL
open science

Effect of Light Intensity and Light Quality on Diatom Behavioral and Physiological Photoprotection

Antoine Prins, Paul Déléris, Cédric Hubas, Bruno Jesus

To cite this version:

Antoine Prins, Paul Déléris, Cédric Hubas, Bruno Jesus. Effect of Light Intensity and Light Quality on Diatom Behavioral and Physiological Photoprotection. Frontiers in Marine Science, 2020, 7, pp.203. 10.3389/fmars.2020.00203 . mnhn-02556040

HAL Id: mnhn-02556040

https://mnhn.hal.science/mnhn-02556040v1

Submitted on 27 Apr 2020

HAL is a multi-disciplinary open access archive for the deposit and dissemination of scientific research documents, whether they are published or not. The documents may come from teaching and research institutions in France or abroad, or from public or private research centers.

L'archive ouverte pluridisciplinaire **HAL**, est destinée au dépôt et à la diffusion de documents scientifiques de niveau recherche, publiés ou non, émanant des établissements d'enseignement et de recherche français ou étrangers, des laboratoires publics ou privés.

frontiers in Marine Science

ORIGINAL RESEARCH
published: 21 April 2020
doi: 10.3389/fmars.2020.00203

Effect of Light Intensity and Light Quality on Diatom Behavioral and Physiological Photoprotection

Antoine Prins[1,2†], Paul Deleris[1], Cédric Hubas[2] and Bruno Jesus[1,3†]*

[1] Mer Molécules Santé EA 2160, Faculté des Sciences et des Techniques, Université de Nantes, Nantes, France, [2] Muséum National d'Histoire Naturelle, FRE BOREA 2030, MNHN-IRD-CNRS-SU-UCN-UA, Station Marine de Concarneau, Concarneau, France, [3] Biosystems & Integrative Sciences Institute, Faculty of Sciences, University of Lisbon, Lisbon, Portugal

In this study, we investigated the different photoregulation responses of diatom dominated natural biofilms to different light intensities and wavelengths, over a tidal cycle in the laboratory. We compared the overall effect of light spectral quality from its light absorption (*Qphar*) dependent effect. Two different conditions were compared to study photoprotective strategies: sediment (migrational) and without sediment (non-migrational). Three different colors (blue, green, and red) and two light intensities (low light, LL at 210 μmol.photons.m^{-2}.s^{-1} and high light, HL at 800 μmol.photons.m^{-2}.s^{-1}) showed strong interactions in inducing behavioral and physiological photoprotection. Non-migrational biofilm non-photochemical quenching (*NPQ*) was much more reactive to blue HL than red HL while it did not differ in LL. We observed a biphasic *NPQ* response with a light threshold between 200 and 250 μmol.photons.m^{-2}.s^{-1} of *Qphar* that elicited the onset of physiological photoprotection. Similar HL differences were not observed in migrational biofilms due to active vertical migration movements that compensated light saturating effects. Our results showed that within migrational biofilms there was an interaction between light quality and light intensity on cell accumulation pattern at the sediment surface. This interaction led to inverse diatom accumulation patterns between blue and red light at the same intensity: LL (blue + 200.67%, red + 123.96%), HL (blue + 109.15%, red + 150.34%). These differences were largely related to the differential amount of light absorbed at different wavelengths and highlighted the importance of using wavelength standardized intensities. Different vertical migration patterns significantly affected the total pigment content measured at the surface, suggesting that cell could migrate downward more than 2 mm as a photoregulatory response. Colloidal carbohydrates patterns paralleled the vertical migration movements, highlighting their possible role in diatom motility. Our data strongly suggests a wavelength and Qphar dependent light stress threshold that triggers upward and downward movements to position microphytobenthic diatoms at their optimal depth.

Keywords: diatoms, fluorescence, PAM, migration, photoprotection

OPEN ACCESS

Edited by:
Wim Vyverman,
Ghent University, Belgium

Reviewed by:
Graham J. C. Underwood,
University of Essex, United Kingdom
Reimund Goss,
Leipzig University, Germany

****Correspondence:***
Antoine Prins
antoine.prins@univ-nantes.fr;
taone@hotmail.fr

† These authors have contributed equally to this work

Specialty section:
This article was submitted to Marine Ecosystem Ecology, a section of the journal Frontiers in Marine Science

Received: *30 November 2019*
Accepted: *16 March 2020*
Published: *21 April 2020*

Citation:
Prins A, Deleris P, Hubas C and Jesus B (2020) Effect of Light Intensity and Light Quality on Diatom Behavioral and Physiological Photoprotection. Front. Mar. Sci. 7:203. doi: 10.3389/fmars.2020.00203

INTRODUCTION

Mycrophytobenthos dominated mudflats are highly productive coastal ecosystems (MacIntyre et al., 1996; Underwood and Kromkamp, 1999) and diatom biofilms forming at the sediment surface during each diurnal tidal cycle are often at the source of this high productivity (e.g., Paterson et al., 2003). These biofilms are also responsible for a range of important biogeochemical processes including sediment stabilization (Paterson, 1989; Yallop et al., 1994), modulation of oxygen availability (Walpersdorf et al., 2017), as well as influencing carbon turnover and availability through the production of polymeric exudates (Perkins et al., 2001; Taylor et al., 2013) which in turns affects microbial diversity (Haynes et al., 2007). Epipelic diatoms, i.e., motile diatoms that move around sediment particles (Round, 1965), exhibit marked vertical movements inside the sediment matrix (Round and Happey, 1965; Consalvey et al., 2004b) that can be divided in two types: an endogenous circadian cycle synchronized with daily emersion periods whereby cells migrate to the sediment surface forming biofilms; and smaller fine tuning vertical adjustments positioning cells at optimal light levels, functioning as a photo-regulation mechanism (Perkins et al., 2001; Jesus et al., 2006; Cartaxana et al., 2011; Serôdio et al., 2012). The circadian rhythms are endogenously controlled and are kept for several days in laboratory conditions without artificial tides and exposed to continuous light (Round and Happey, 1965; Paterson, 1986; Serôdio et al., 1997; Mitbavkar and Anil, 2004; Coelho et al., 2011). The smaller photo-regulation movements are one of the main photo-regulation mechanisms of epipelic diatoms (Jesus et al., 2009; Perkins et al., 2010; Cartaxana et al., 2011; Laviale et al., 2016), while epipsammic diatoms (strongly associated to sediment grains) depend mainly on the thermal dissipation of excessive light energy through the xanthophyll cycle (XC) to photo-regulate (Cartaxana et al., 2011; Barnett et al., 2015; Blommaert et al., 2018). The XC relies on the presence of a transthylakoidal proton gradient to de-epoxidise diadinoxanthin (Diad) into its energy-dissipation form diatoxanthin (Diat). It presumably induces a conformational shift in the light harvesting antennas that leads to excess energy being dissipated by heat through a non-photochemical quenching (NPQ) process (e.g., Olaizola and Yamamoto, 1994; Lavaud et al., 2004; Lavaud and Goss, 2014). Several studies have tried to quantify the relative importance of the two photo-regulation mechanisms (e.g., Perkins et al., 2010; Serôdio et al., 2012), notably by using migration inhibitors (Cartaxana and Serôdio, 2008) to separate the photo-regulatory effect of the XC from the vertical movements. Overall, published data shows that microphytobenthos depend on both photo-regulation mechanisms but that the two strategies are strongly dependent on their life forms (i.e., epipelic vs. epipsamic) (Cartaxana et al., 2011; Barnett et al., 2015). A few studies have investigated the trade-off between vertical migration (VM) and NPQ (Perkins et al., 2010; Serôdio et al., 2012; Barnett et al., 2015; Laviale et al., 2016; Blommaert et al., 2018). Diatoms movements have been differentiated in phototaxis and photokinesis (Nultsch, 1971; Häder, 1986). The former describing an oriented movement toward or away from a light source and the latter describing the speed of the movement as a response to light fluence rate (McLachlan et al., 2009). Both positive and negative phototaxis, toward and away from light, have been reported for different diatoms and different light intensities (Nultsch, 1971; Cohn et al., 1999; Du et al., 2010; Ezequiel et al., 2015). Benthic diatoms, in the absence of light cues, may also exhibit negative gravitaxis inducing upward movements to the sediment surface (Frankenbach et al., 2014). Most studies on diatom movement, growth and photosynthetic properties have investigated the effect of light intensity regardless of light spectra (Perkins et al., 2001; Paterson et al., 2003; Underwood et al., 2005; Jesus et al., 2006; Chevalier et al., 2010; Jauffrais et al., 2015). Light intensity is a wavelength weighted energy measurement that refers to the total number of photons received per unit area in a given time. Its use has been widely spread in photosynthetic studies because photosynthetic photochemical reactions are driven by total amount of photon received rather than the amount of energy received by each photon (Kume, 2018). In the aforementioned studies (Perkins et al., 2001; Paterson et al., 2003; Underwood et al., 2005; Jesus et al., 2006; Chevalier et al., 2010; Jauffrais et al., 2015) light has been integrated over the photosynthetic active radiation (PAR) spectrum, not accounting for the spectral variations within the light spectrum. However, these changes in light composition can affect diatom photo-protective capacity and photo-acclimation to high light intensities (Phaeodactylum tricornutum) (Schellenberger Costa et al., 2013a; Brunet et al., 2014). Light composition can also affect locomotion speed thereby affecting diatom vertical migration (Wenderoth and Rhiel, 2004; McLachlan et al., 2009). Spectral differences affect the relative proportion of photons available at each wavelength per unit area in a given time. In turn this modify on one hand the total amount of energy and on the other hand specific interactions, i.e., absorptions, with different structures such as diatoms' pigments and chromophores. It is unknown whether light quality changes only modulate the amount of light being absorbed by diatoms or if there are other effect, possibly due to differential energy levels and other confounding factors. To differentiate between chromatic differential absorption and other effects we compared intensity with Qphar (Gilbert et al., 2000) which is the photosynthetically absorbed radiation weighing in specific absorption coefficients of the major pigments. Currently, no studies exist on the effect of light quality regarding the two main diatom photo-regulation mechanisms. The objective of the current study was to investigate the effect of light spectral composition and light intensity on diatom physiological and behavioral photo-regulation mechanisms throughout a tidal cycle, using MPB assemblages in natural sediment and assemblages immobilized on petri dishes. Light quality effects will firstly be studied from an intensity perspective before considering their effect from an absorbance point of view.

MATERIALS AND METHODS

Site and Sampling

The sampling site was located in La Couplasse mudflats (Bourgneuf Bay, 47.015753, −2.024148) and sampling was

carried out on February 2018 during low tide. It is a non-protected area that did not require a permit for this kind of biological material sampling. Superficial sediment (upper 5 mm) was scrapped and transported back to the laboratory where it was spread out evenly in trays and submerged with water from the site in a room with natural lighting, allowing for the reconstitution of the biofilm the next day. The sediment at this site is dominated by benthic epipelic diatoms (e.g., Hernández Fariñas et al., 2017).

Experimental Setup

Water was drained from the trays on the day after the sampling and 3 h prior to the expected low tide we added two layers of lens tissue on top of the sediment. The sediment was then exposed to natural light from a window to facilitate biofilm vertical migration. Lens tissues were recovered at the middle of the virtual emersion time (low-tide peak), thereby harvesting the microalgae that had migrated to the sediment surface during the first 3 h (Eaton and Moss, 1966). Cells were extracted from the lens tissues by gently scrapping them into site-filtered sea water and kept in darkness before further use. On the second day, 5 h before expected low tide and 2 h before the beginning of the experiment 48 black microplates wells (22 mm diameter and 18 mm depth) were filled with either the same mud used for extraction or clean lens tissue inoculated with algal suspension. Mud samples contained both migratory and non-migratory diatoms from the field. Half were filled with one lens tissue layer and inoculated with 2 mL of algal suspension; the other half was filled with mud (15 mm) and 0.5 mL of algal suspension. To facilitate handling the 12 wells microplates were cut in rows of 4 wells containing each 3 replicates and a dark control (**Figure 1**). Mud and lens tissue samples will henceforth respectively be referred as migrational and non-migrational biofilms.

Light Treatments

LEDs light sources (SL 3500 – PSI) were calibrated with a light sensor (MSC15 – Gigahertz-Optik) to deliver 800 μmol.photons.m^{-2}.s^{-1} from a 30 cm distance onto the microplates. Three monochromatic lights were used to set up three light conditions: Red (635 nm, FWHM 20 nm), Green (528 nm, FWHM 34 nm) and Blue (444 nm, FWHM 20 nm). To produce low intensities condition neutral filters were applied on each color to reduce light intensity to 210 μmol.photons.m^{-2}.s^{-1}. Dark condition was obtained by covering microplate wells with dark tape. All treatments were replicated three times.

PAM Chlorophyll Fluorescence

Fluorescence was measured with an imaging-PAM (WALZ – Germany) using blue Luxeon LEDs (450 nm) for both actinic illumination and saturating pulses. Absorptivity was measured with the same instrument using a different set of incorporated LEDs, red (660 nm) and infrared (780 nm) performing a pixel by pixel comparison of images recorded under the two lights using the equation: Absorptivity = 1 – (Red/Infrared). The microplates were placed at 20 cm from the camera (CCD IMAG-K4) to optimize lens focus and illumination. Fluorescence measurements consisted of rapid light curves (RLC) from which all photosynthetic parameters were calculated. RLCs were carried in sequences, starting with migrational 800 μmol.photons.m^{-2}.s^{-1} RGB followed by non-migrational 800 μmol.photons.m^{-2}.s^{-1} RGB then migrational 210 μmol.photons.m^{-2}.s^{-1} RGB and finally non-migrational 210 μmol.photons.m^{-2}.s^{-1} RGB. The time elapsed between the first and last measurement was 25 min. The first RLC measurement (T0) was done 3 h before expected low tide and in darkness, it was followed by three time measurements: T1, done 1.5 h before low tide and after 1.5 h of illumination; T2, synchronized with low tide and after 3 h of illumination; and T3, 1.5 h after low tide with 4.5 h of illumination. RLCs consisted of 12 lights levels (0, 4, 18, 41, 74, 142, 279, 518, 745, 986, 1302, 2342 μmol.photons.m^{-2}.s^{-1}) with 30 s steps. RLC parameters α-slope and *rETRm* were estimated by fitting Silsbe and Kromkamp (2012) modified equation of Eilers and Peeters (1988).

$$\phi II_i = \frac{Fm' - F'}{Fm'} \quad (1)$$

$$\phi II\,(E) = rETRm + \alpha - \text{slope} + \frac{\alpha - \text{slope}}{E * Eopt * (Eopt * E - 2)} \quad (2)$$

Where F' and Fm' are respectively the fluorescence yield under actinic light and the maximum fluorescence yield after a light saturating pulse at each RLC step; E is the light intensity in μmol.photons.m^{-2}.s^{-1}; ϕII_i is the photosystem II effective quantum efficiency at each i steps of the RLC. ϕII_1 correspond to the optimal photosystem II quantum efficiency measured during the first step of the RLC. $\phi II(E)$ refers to light-dependent changes of ϕII. From fitting $\phi II(E)$ the following photosynthetic parameters were estimated: the initial slope of the RLC (α-slope) under limiting irradiance, the maximum relative electron transport rate of the RLCs (*rETRm*) and the optimal light parameter (*Eopt*) of ϕII versus E curves. *Eopt* corresponds to the irradiance (μmol.photons.m^{-2}.s^{-1}) at which ETR saturates and where further increment of light induces photoprotection. Continuous light exposure prevented measurements of the fully oxidized photosystem II at the different time of the tide. In these conditions direct NPQ measurements proved to be impractical due to the cofounding effect of NPQ relaxation and migration. Instead α-slope was used as a proxy for NPQ induction and relaxation. It has been shown to be inversely proportional to NPQ allowing to trace short-term changes in NPQ levels without dark incubation (Cruz and Serôdio, 2008).

Pigments

At the end of the experiment (T3) the migrational samples were sampled by freezing with liquid nitrogen and contact cores (1 cm diameter and 2 mm deep). They were then stored in a −80°C freezer and freeze dried before further processing. Pigment extraction was performed in a dark chamber using acetone (90%), sonicated for 90 s, followed by overnight extraction at 4°C. HPLC analysis was performed according to Van Heukelem method (Heukelem and Thomas, 2001) using a 1 ml/min flow for 36 min with methanol (solvent B) and

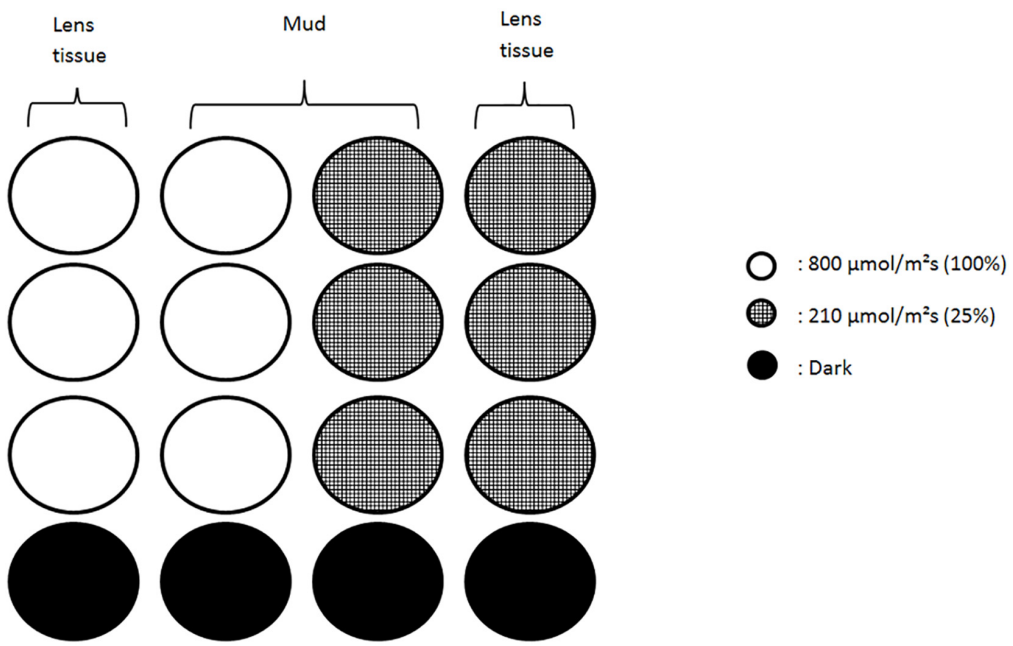

FIGURE 1 | Schematic of the wells set up under each color. Each column of four wells was independently bound and contained three replicates and a dark control. Lens tissue wells were filled with a suspension of migrating diatoms collected from the mud. Wells with mud contained natural assemblages of algae/diatom dominated by epipelic species. Low light conditions (210 µmol.photons.m^{-2}.s^{-1}) were obtained using neutral filters.

methanol/TBAA-28 mM (70/30 – solvent A) going from 5 to 95% of solvent B and vice versa for solvent A. Injection volume was 100 µL with 28.5 µL sample and 71.5 µL TBAA 28 mM. An Agilent Eclipse XDB-C8 column was used at 60°C. Detection was done at 450 and 665 nm using a diode array detector. Approximately 0.17 g of sediment and 1.5 ml of solvent were used for each sample. Identification and pigment concentrations were calibrated using the response factors (RF) of pigments standards (DHI-Danemark). Data analysis was conducted on relative percentage of pigments. The de-epoxidative state (DES) was calculated as Diat/(Diat + Diad). Pigment determination was not performed on non-migrating biofilms due to lack of biological material for the different analysis.

Absorption Spectra

To compare whether differences in light color responses were due to total light absorbed or other chromatic effect a pigment weighted light absorption (*Qphar*) was calculated. *Qphar(λ)* correspond to the amount and proportion of light absorbed by the cells at different wavelengths. It is calculated according to a modified Eq. (4) of Gilbert et al. (2000). The specific *in vitro* absorption coefficients of microphytobenthos samples a_{mpb} were reconstructed according to Eq. (3).

$$a_{mpb}(\lambda) = \sum_{i}^{n} a_i(\lambda)^* C_i \quad (3)$$

$$Qphar(\lambda) = Q(\lambda) - (Q(\lambda)^* e^{-a_{ph}(\lambda)}) \quad (4)$$

$a(\lambda)$ is the concentration specific absorption coefficient in m^2g^{-1}, its values were obtained from the literature (Clementson and Wojtasiewicz, 2019). *C* is the pigment specific average concentration within all contact cores in mg.g^{-1}. *Q(λ)* is the photosynthetically available radiation at the top of the sediment or in lens tissue in µmol.photons.m^{-2}.s^{-1}. Pigments used for reconstruction of the light absorption spectrum were chlorophyll *a*, chlorophyll *c2*, fucoxanthin, β-carotene, diadinoxanthin and diatoxanthin.

Carbohydrates and Proteins

At T3, migrational and non-migrational samples were frozen and stored at −80°C for carbohydrate and protein quantification. Colloidal (soluble) fractions were extracted from thawed samples. They were first mixed in 2 mL of artificial sea water for 1.5 h (Orbital shaker, YELLOWline), then the supernatant was removed and the remaining sediment was mixed again with 2 mL of artificial sea water and 300 mg of Dowex Marathon Cex change resin to extract the bound (attached to sediment particles) fraction. Carbohydrate and protein quantification were done by spectroradiometry (Genesys 10S Uv/Vis) using the colorimetric reactions methods of DuBois et al. (1956) for carbohydrates and a modified Lowry method for proteins (Frølund et al., 1996).

Species Identification

Algal suspensions were preserved with glutaraldehyde (4%) and sediment cores were frozen with liquid nitrogen, respectively stored at 4 and −80°C. Three vials were filled with 1.5 mL of algal suspension while sediment cores were first placed in ludox (®HS-40 coloidal silica) to separate cells from the

sediment and were then resuspended in a known volume of water and cleaned up following the protocol by Consalvey (2002). Succinctly, it consisted of a 24 h oxidation in saturated potassium permanganate solution, followed by the addition of hydrochloric acid for 2 h at 70°C. Lastly, cells were rinsed seven times with ultrapure water in a final volume of 1.5 mL. A 50 μl subsample was permanently mounted on microscope slides using NaphraxTM. Cell counting, observation and identification of diatom valves were made with an optical microscope (Olympus). At 1000 magnification, 10 zones were chosen using randomly generated numbers and counted in five different slides until more than 400 individuals were counted. Identification was performed using the literature (Paulmier, 1997; Ribeiro, 2010; Mertens et al., 2014). Biovolumes were retrieved from the literature (Olenina et al., 2006; Ribeiro, 2010) and calculated according to morphologically based equations (Hillebrand et al., 1999; Olenina et al., 2006).

Statistical Analysis

All statistical analyses were performed using R (R Core Team, 2017). Two-ways analysis of covariance (ANCOVA) were performed to compare datasets possessing a time variable with a linear regression. This comprised analysis of absorptivity, ϕII_1 and α-slope over time for the different treatments of either same color or same light intensity. Pigment compositions were tested using a permutational multivariate analysis of variance using distance matrices based on Bray–Curtis dissimilarity index. Multivariate homogeneity of group dispersions was tested with a permutation-based test. Pigment and EPS differences between treatments were tested using two-way analysis of variance (ANOVA), after normality and homogeneity of variance had been verified using Shapiro–Wilk and Barlett tests, respectively. Individual differences were tested using *Post hoc* Tukey HSD tests. A principal components analysis (PCA) was used to visualize the pigment variance between treatments.

RESULTS

Species Composition

The dominant species in the non-migrational biofilms were: *Navicula meulemansii* (71.8%), *Navicula spartinetensis* (17.3%), *Gyrosigma limosum* (5.3%), *Gyrosigma wansbecki* (3.8%), and *Pleurosigma angulatum* (1.3%) (**Figure 2**). The migrational biofilm was dominated by *Navicula meulemansii* (30.42%), *Thalassiosira* cf. *proschkinae* (11.47%), *Navicula spartinetensis* (10.7%), *Gyrosigma limosum* (7.0%), *Gyrosigma wansbeckii* (5.7%), *Thalassiosira* cf. *pseudonana* (4.5%), *Odontella aurita* (3.74%), *Raphoneis amphiceros* (2.49%), *Tryblionella* sp. (2.0%), *Coconeis speciosa* (2.0%), *Nitzschia* cf. *lorenziana* (2.0%), *Thalassiosira* cf. *angulata* (1.7%), *Pleurosigma angulatum* (1.7%) (**Figure 2**).

Photosynthetic Activity as a Function of Color-Dependent Light Intensity (Qphar)

Photosynthetic active radiation intensity is a widely used measure of standardized light dosage that can be compared across a variety of experiments. However, when light spectral composition is taken into account this measurement becomes flawed due to the fact that photosynthetic organisms absorb light differently, depending on their pigment composition. Thus direct comparisons of similar light intensities at different wavelengths are hindered by potentially different photoprotective reactions. Recalculating the total intensity absorbed at each wavelength (*Qphar*) produced six different intensities. These Qphar intensities were respectively 63.8 (R210), 76.2 (G210), 198.3 (B210), 255.02 (B800), 305.01 (G800) and 793.29 (B800) μmol.photons.m^{-2}.s^{-1} (**Figure 3**). Migrational and non-migrationnal biofilms (**Figure 3**) displayed a Qphar threshold where alpha values switched from a NPQ relaxation state to a light induced NPQ production. Alpha is inversely proportional to NPQ intensity and a characteristic shift from values over 100% to values below 100% indicated a threshold where light started inducing physiological photoprotection throught NPQ increase. This threshold was observed between 200 and 250 μmol.photons.m^{-2}.s^{-1} of Qphar (**Figure 3**) effectively separating our treatments in low light (LL) when it is below 200 μmol.photons.m^{-2}.s^{-1} and high light (HL) when above 250 μmol.photons.m^{-2}.s^{-1} of Qphar.

Vertical Migration Absorptivity Changes at the Surface

Absorptivity increased over time in all treatments subjected to light and decreased in the dark control (**Figure 4**). Light intensity had a significant effect on the absorptivity changes in red, blue and green wavelengths (ANCOVA, $p < 0.05$). Time also had a significant effect on absorptivity changes in red, green, blue, and dark treatments (ANCOVA, $p < 0.05$), with no significant interaction between time and light intensity. Within each set of light intensities there was also a significant effect of light color (ANCOVA, $p < 0.001$), and light color over time (ANCOVA, $p < 0.05$) which differed in the two conditions (HL and LL). Red and blue treatments showed different effects at the two light intensities, with blue absorptivity increasing 101% in LL and only 9% in HL; while red absorptivity increased 50% in HL and only 24% in LL (**Figure 4**). The dark control showed a decrease in absorptivity over time.

Optimal PSII Quantum Efficiency (ϕII_1)

On average, optimal PSII quantum efficiency (ϕII_1) in a dark adapted state at T0 were significantly higher ($p < 0.001$ *t*-test) for migrational biofilms (mean = 0.607) than non-migrational biofilms (mean = 0.401). Non-migrational treatments were characterized by a ϕII_1 increase in LL and ϕII_1 decrease in HL, with significant effects of time (ANCOVA, $p < 0.01$), light intensity (ANCOVA, $p < 0.001$) and intensity over time (ANCOVA, $p < 0.001$). Non-migrational biofilms ϕII_1 was affected differently by the light color in LL and HL treatments (**Figure 5**). With the exception of dark and red, ϕII_1 in HL showed significant differences between colors ($p < 0.001$), time ($p < 0.001$) and color over time ($p < 0.001$). Contrastingly, ϕII_1 in LL samples increased significantly over time ($p < 0.001$) and remained constant in dark controls. There were no significant

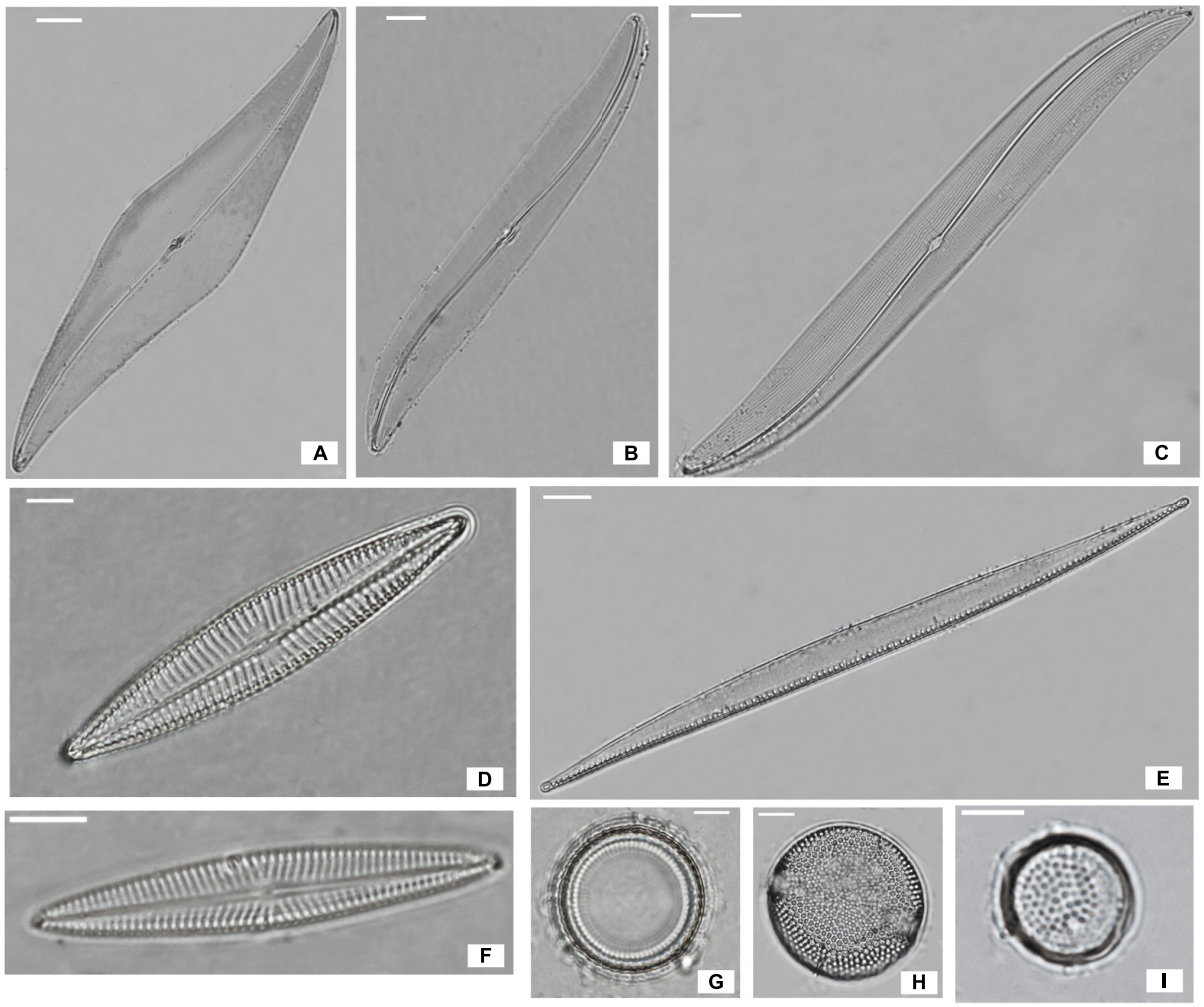

FIGURE 2 | Most abundant diatoms species of Bay de Bourgneuf site; **(A)** *Pleurosigma angulatum* (scale bar = 20 μm); **(B)** *Gyrosigma limosum* (5 μm); **(C)** *Gyrosigma wansbecki* (10 μm); **(D)** *Navicula spartinetensis* (5 μm); **(E)** *Nitzschia* cf. *lorenziana* (10 μm); **(F)** *Navicula meulemansii* (5 μm); **(G)** *Thalassiosira* cf. *pseudonana* (5 μm); **(H)** *Thalassiosira* cf. *angulata* (5 μm); **(I)** *Thalassiosira* cf. *proschkinae* (5 μm).

differences in LL ϕII_1 between colors and colors over time (**Figure 5**). ϕII_1 of all migrational biofilms increased in LL and decreased in HL, with significant effects of time ($p < 0.001$), intensity ($p < 0.001$), and intensity over time ($p < 0.001$) (**Figure 5**). All migrational HL biofilms (apart from control) showed a significant ϕII_1 decrease over time ($p < 0.001$) and no significant differences between colors and colors over time. With the exception of green and blue samples, the LL migrational ϕII_1 differed significantly between color treatments with significant effect of color ($p < 0.001$), time ($p < 0.05$), and color over time ($p < 0.01$).

RLC Parameters

Changes in α-slope were strongly correlated with ϕII_1 (Pearson correlation of 0.99, $p < 0.001$) with α-slope increasing in all LL treatments and decreasing in all HL treatments over time (**Tables 1**, **2**). There was a significant effect of light intensity and light color in all α-slope values that were always significantly different from the dark controls over time (ANCOVA, $p < 0.001$) (**Figure 6**). α-slope significantly decreased with time in HL migrational biofilms and significantly increased with time in migrational LL biofilms (ANCOVA, $p < 0.001$), with no significant differences between color and light color over time (**Figure 6**). In migrational LL biofilms only red samples showed significantly higher α-slope values than the other two colors (ANCOVA, $p < 0.05$). The biggest significant difference in α-slope values was observed in non-migrational HL samples were α-slope significantly decreased between colors ($p < 0.001$), over time ($p < 0.001$) and between colors over time ($p < 0.001$) (**Figure 6**).

Changes in *rETRm* over the course of the experiment were strongly influenced by light color and light intensity (**Tables 1**, **2**). In all samples and all conditions *rETRm* systematically increased from T0 to T1 and then depending on the conditions either continuously decreased or increased. LL non-migrational biofilm was the only condition where *rETRm* kept increasing throughout

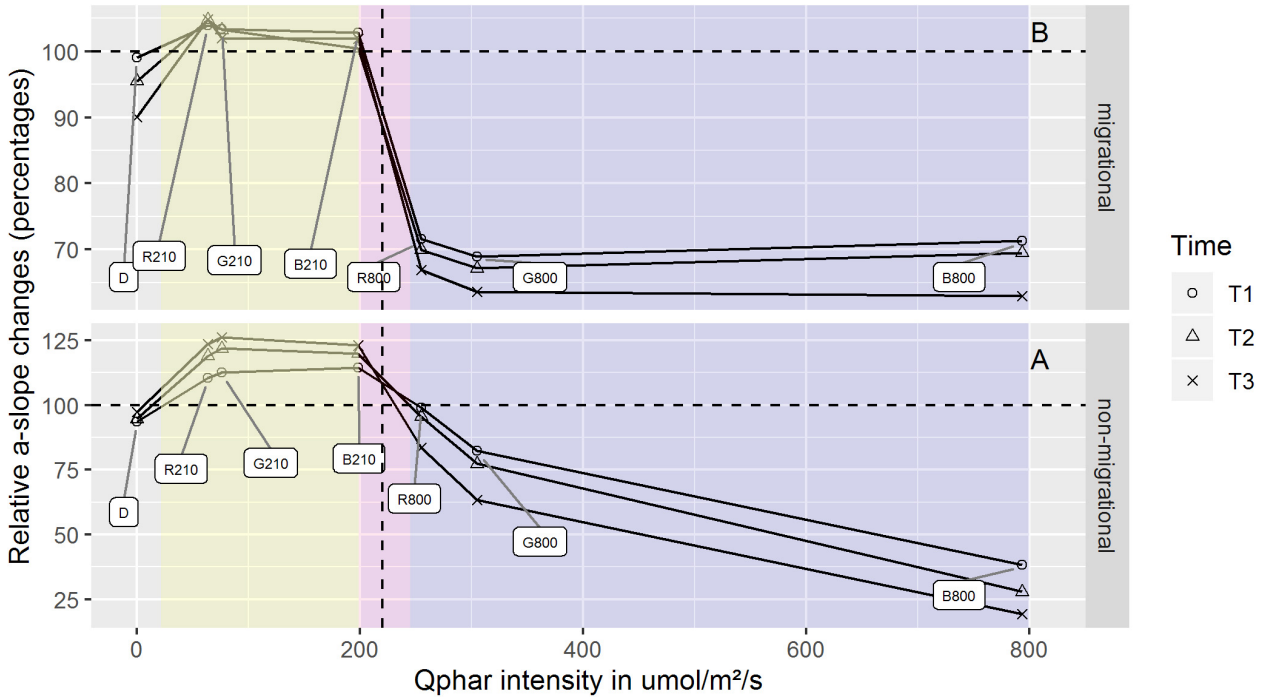

FIGURE 3 | α-slope changes for differing Qphar intensities. α-slope are displayed as percentages of the initial value prior to illumination. Qphar recalculated intensities are 63.8 (R210), 76.2 (G210), 198.3 (B210), 255.02 (R800), 305.01 (G800), and 793.29 (B800) μmol.photons.m^{-2}.s^{-1}. The area below 200 μmol.photons.m^{-2}.s^{-1} (yellow) correspond to non-stressful light conditions where NPQ is relaxing while the area above 250 μmol.photons.m^{-2}.s^{-1} (purple) correspond to stressful light inducing NPQ. The boundary and threshold between LL Qphar and HL Qphar is represented in pink. n = 3 for each point.

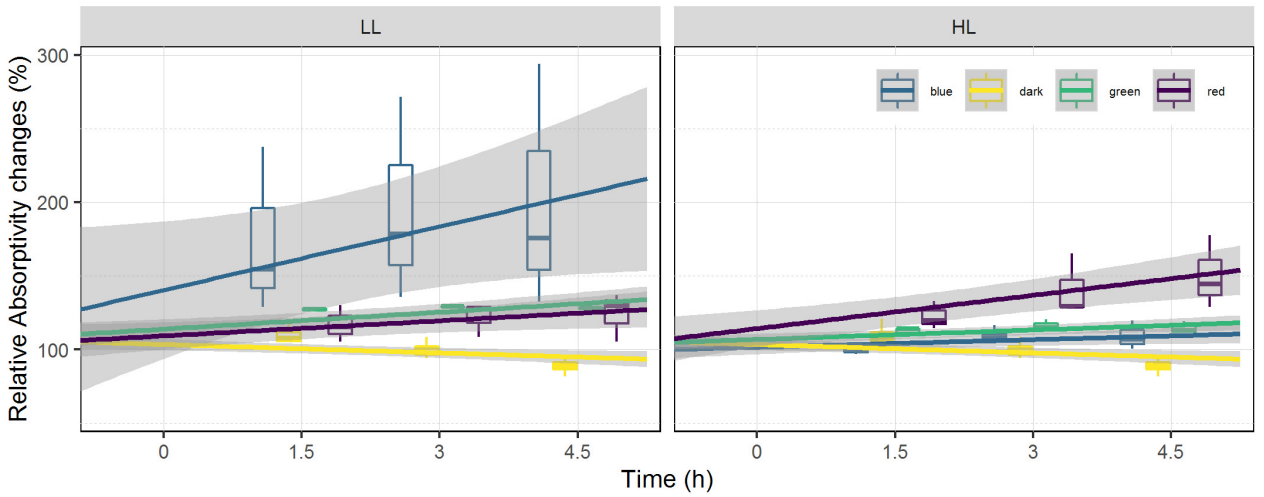

FIGURE 4 | Relative absorptivity changes at the surface of the sediment. Absorptivity is displayed as percentage of the initial value prior to illumination (at T0). It is used as a biomass proxy at the surface of the sediment. Each color has been fitted with a linear model where confidence interval (0.95) are represented in gray (n = 3).

the whole experiment (with the exception of blue T3). *rETRm* color treatments were significantly higher than dark controls ($p < 0.01$) while not significantly differing between each color. On the contrary in HL all treatments significantly differed ($p < 0.01$) with the exception of red and dark. At the end of the light exposure in non-migrational biofilms there was a significant effect of intensity ($p < 0.001$) on *rETRm* values exemplified by a 44% decrease in blue HL and a 224% increase in LL compared to initial values. In all migrational biofilms *rETRm* increased to their maximum value at T1 and then slowly decreased over

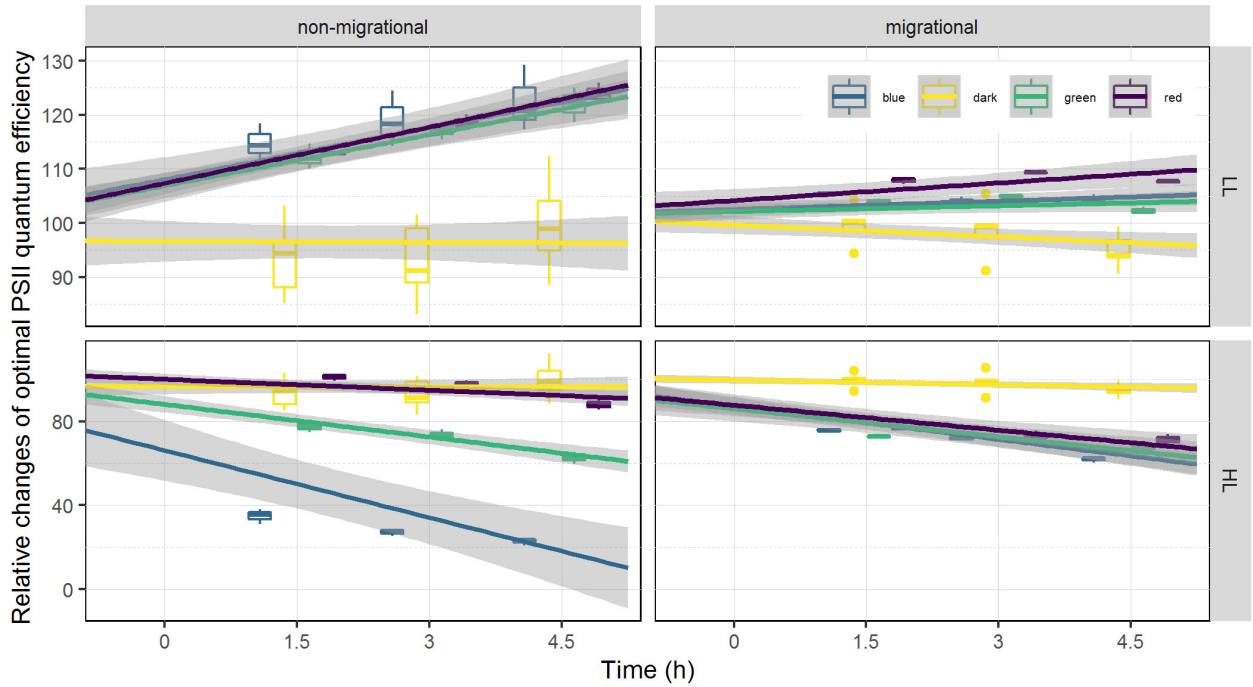

FIGURE 5 | Relative changes of optimal photosystem two light efficiency ϕII_1. ϕII_1 is displayed as percentage of the initial value prior to illumination (at T0). Each color has been fitted with a linear model where confidence interval (0.95) are represented in gray (n = 3).

TABLE 1 | Photosynthetic parameters and ϕII_1 values obtained from rapid light curve fitting of ϕII(E) within the non-migrational biofilm.

		Blue		Dark	Green		Red	
µmol.photons.m^{-2}.s^{-1}		**800**	**210**	**NA**	**800**	**210**	**800**	**210**
α-slope	T0	0.38 ± 0.002	0.39 ± 0.01	0.37 ± 0.017	0.37 ± 0.01	0.37 ± 0.01	0.37 ± 0.004	0.37 ± 0.011
	T1	0.15 ± 0.012	0.44 ± 0.003	0.34 ± 0.007	0.31 ± 0.003	0.42 ± 0.011	0.37 ± 0.004	0.41 ± 0.01
	T2	0.11 ± 0.007	0.46 ± 0.008	0.34 ± 0.01	0.29 ± 0.004	0.45 ± 0.007	0.35 ± 0.004	0.44 ± 0.01
	T3	0.07 ± 0.007	0.48 ± 0.008	0.36 ± 0.014	0.24 ± 0.007	0.47 ± 0.004	0.31 ± 0.007	0.46 ± 0.008
ϕII	T0	0.41 ± 0.002	0.42 ± 0.012	0.4 ± 0.019	0.4 ± 0.013	0.4 ± 0.012	0.39 ± 0.004	0.4 ± 0.012
	T1	0.14 ± 0.015	0.48 ± 0.004	0.37 ± 0.024	0.31 ± 0.004	0.45 ± 0.011	0.4 ± 0.007	0.45 ± 0.014
	T2	0.11 ± 0.006	0.5 ± 0.008	0.37 ± 0.015	0.29 ± 0.002	0.47 ± 0.008	0.38 ± 0.002	0.47 ± 0.013
	T3	0.09 ± 0.006	0.51 ± 0.011	0.39 ± 0.018	0.25 ± 0.008	0.49 ± 0.002	0.35 ± 0.007	0.49 ± 0.008
rETRm	T0	40.8 ± 3	45.7 ± 3	39.2 ± 7.5	38.8 ± 2	41.4 ± 3	33.6 ± 2	38.7 ± 3
	T1	52.7 ± 7	98.4 ± 1	65.35 ± 10.5	79.3 ± 3	86.5 ± 7	73.2 ± 2	75.5 ± 6
	T2	30.8 ± 5	110 ± 5	74.45 ± 8.5	67.8 ± 3	102.9 ± 7	70.2 ± 1	88.7 ± 7
	T3	17.8 ± 1	104.1 ± 5	77.45 ± 11.5	45.3 ± 2	103.7 ± 4	49.3 ± 2	92.9 ± 5

Equation derived from Silsbe and Kromkamp (2012) modified equation of Eilers and Peeters (1988). The entire well was used as a region of interest. n = 3. ± : standard deviations.

time. Only red light displayed a significant *rETRm* difference between intensities ($p < 0.05$). Overall blue light treatments had a significant higher *rETRm* than samples of the same intensity with the exception of red LL.

Pigments and EPS

Mean total pigment content is a proxy of the biomass within the 2 upper mm (**Figure 7**). At T3 the mean total pigment content (**Figure 7**) resembled the patterns observed in absorptivity measured at T3 (**Figure 4**) that were marked by an interaction of light quality and light intensity ($p < 0.05$), producing opposite effects at LL and HL. In the LL treatment, the highest mean total pigment content was found under blue light while the lowest content was found in red. The opposite trend was observed in HL with the highest mean total pigment content observed under red light and lowest in blue light.

The average pigment composition of migrational biofilms at the end of the experiment was: chlorophyll *a* (Chl *a*, 40.8%), fucoxanthin (Fuco, 37.8%), diadinoxanthin (Diad, 8.8%), chlorophyll *c1* (Chl *c1*, 3.8%), diatoxanthin (Diat, 2.54%),

TABLE 2 | Photosynthetic parameters and ϕII_1 values obtained from rapid light curve fitting of ϕII(E) within the migrationnal biofilm.

		Blue		Dark	Green		Red	
μmol.photons.m^{-2}.s^{-1}		**800**	**210**	**NA**	**800**	**210**	**800**	**210**
α-slope	T0	0.59 ± 0.006	0.59 ± 0.003	0.57 ± 0.009	0.59 ± 0.003	0.59 ± 0.002	0.57 ± 0.003	0.58 ± 0.002
	T1	0.42 ± 0.005	0.6 ± 0.004	0.57 ± 0.0145	0.41 ± 0.004	0.61 ± 0.008	0.41 ± 0.003	0.6 ± 0.005
	T2	0.41 ± 0.006	0.59 ± 0.004	0.55 ± 0.018	0.4 ± 0.006	0.61 ± 0.001	0.4 ± 0.01	0.61 ± 0.003
	T3	0.37 ± 0.007	0.6 ± 0.006	0.52 ± 0.014	0.38 ± 0.006	0.6 ± 0.005	0.38 ± 0.012	0.61 ± 0.004
ϕII	T0	0.61 ± 0.007	0.61 ± 0.002	0.6 ± 0.01	0.61 ± 0.005	0.62 ± 0.002	0.59 ± 0.001	0.61 ± 0.001
	T1	0.46 ± 0.009	0.65 ± 0.004	0.6 ± 0.025	0.45 ± 0.002	0.64 ± 0.005	0.45 ± 0.004	0.65 ± 0.005
	T2	0.44 ± 0.011	0.64 ± 0.003	0.59 ± 0.033	0.43 ± 0.004	0.65 ± 0.001	0.43 ± 0.012	0.66 ± 0.001
	T3	0.38 ± 0.01	0.64 ± 0.007	0.57 ± 0.022	0.41 ± 0.005	0.63 ± 0.004	0.42 ± 0.015	0.65 ± 0.003
rETRm	T0	126.3 ± 7	135.9 ± 6	132.55 ± 6.5	131.5 ± 5	138 ± 5	122.5 ± 6	135.5 ± 3
	T1	207.6 ± 18	221 ± 16	172.95 ± 16.5	168.9 ± 1	200.6 ± 10	155.1 ± 5	200.6 ± 6
	T2	189.9 ± 21	188.5 ± 21	169.4 ± 15.5	153.4 ± 5	169.3 ± 12	133.5 ± 9	182.8 ± 7
	T3	184.6 ± 23	171.1 ± 22	159.35 ± 9.5	144.1 ± 5	147.9 ± 12	121.4 ± 10	166.4 ± 7

Equation derived from Silsbe and Kromkamp (2012) modified equation of Eilers and Peeters (1988). The entire well was used as a region of interest. n = 3. ± : standard deviations.

chlorophyll *c2* (Chl *c2*, 2%), alpha and beta-carotene (αβ car, 1.9%), chlorophyll *b* (chl *b*, 1%) and antheraxanthin (anth, 0.8%). Color, light intensity and their interaction had a significant effect ($p < 0.001$) on the relative percentage of pigments (**Figure 8**). The PCA results (**Figure 8**) show that the two main axes explained 57.5% of the variance between pigments, with color treatments aligned along the two axes. Light intensity accounted for 23.1% of the total variance (Between Class Analysis) with significant percentage differences in Diat ($p < 0.001$), Diad ($p < 0.01$), Fuco ($p < 0.01$), and Chl c1 ($p < 0.01$). A *post hoc* test showed a higher percentage of Diat ($p < 0.001$) in all HL treatments (**Figure 8**).This was further exemplified by the significant higher ($p < 0.001$) DES (**Table 3**) in HL compared to LL. Color treatments accounted for 27.4% of the total variance with significant pigment percentage differences of Chl a ($p < 0.001$), Fuco ($p < 0.001$), Anth ($p < 0.001$), Diad ($p < 0.01$), and Diat ($p < 0.01$). *Post hoc* tests showed significant higher Chl a pigment percentage in blue treatments compared to red ones ($p < 0.001$) and higher Fuco percentage in red light ($p < 0.05$) compared to the other two colors. The interaction effect of color and intensity accounted for 67.3% of the total variance with significant pigment percentage differences of Fuco ($p < 0.01$), Diad ($p < 0.01$), Anth ($p < 0.05$), Diat ($p < 0.01$), Chl *a* ($p < 0.05$). Amongst these interaction effects there was a significantly lower Diat ($p < 0.01$) in blue HL compared to the other two colors.

Non-migrational biofilms showed significant differences in colloidal carbohydrates (CC) with higher CC content observed in HL ($p < 0.05$) (**Figure 9**). In HL, there was no significant difference between colors for any carbohydrate fraction nevertheless the variance was very high in blue and red CC. Overall, the carbohydrate contents measured in non-migrational biofilms were very small, which led to values below the detection threshold in bound carbohydrates (BC) and to high variability in CC. There were no significant differences between treatments and controls for all protein measurements *(data not shown)*. The average protein concentration was 0.0114 (± 0.0025) μg.mm^{-2} for non-migrational biofilms and 0.0608 (± 0.010) μg.mm^{-2} for migrational biofilms.

Migrational biofilm CC contents were significantly different between color ($p < 0.001$), light intensity ($p < 0.05$) and their interaction ($p < 0.05$) (**Figure 9**). All color treatments with the exception of red LL had significantly higher CC contents than the dark controls ($p < 0.05$). The interaction effect led to contrasting results at the different light intensities with no significant CC differences between colors in HL while at LL lower CC concentrations were observed in red in comparison to blue ($p < 0.01$). The BC concentrations of the migrational biofilms were also significantly affected by color ($p < 0.001$), with blue treatment having higher BC contents than dark control ($p < 0.05$) in both LL and HL while red treatment only had a higher BC contents than dark control under HL intensities ($p < 0.05$).

DISCUSSION

Both light intensity and light quality had a significant effect on diatom photo-regulation mechanisms (migration and NPQ), with clear differences being observed between migrational and non-migrational biofilms, confirming that vertical migration movements within the sediment matrix plays a major role in diatom photo-regulation.

Species Composition

The diatoms that were present in both migrational and non-migrational biofilms were typical epipelic diatoms from the Bourgneuf bay site, similar to the assemblages observed by Méléder et al. (2007). *Navicula spartinetensis* is found exclusively in intertidal muddy sediments and is one of the most commonly found epipelic species in European Atlantic coasts (Ribeiro, 2010). The only species that had not yet been described for this site was *Navicula meeulmansii*. However, *N. meeulmansii* has only recently been described as a cosmopolitan species tolerating wide range of salinities (Mertens et al., 2014), which

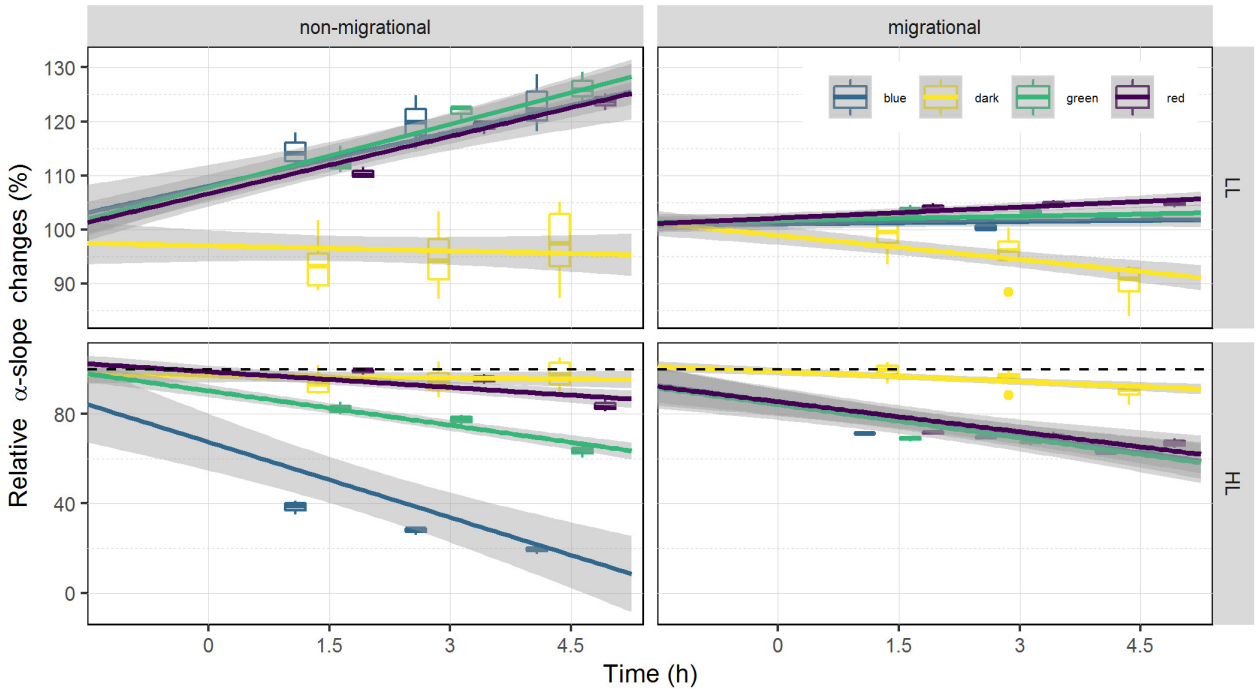

FIGURE 6 | Relative changes of α-slope. α-slope is displayed as percentage of the initial value prior to illumination (at T0). α-slope variations is used as a proxy of NPQ as it is inversely proportional. Each color has been fitted with a linear model where confidence interval (0.95) are represented in gray (n = 3).

may have been previously described as *Navicula phyllepta* or *Navicula microdigitoradiata* in the other studies from this ecosystem (Méléder et al., 2007; Hernández Fariñas et al., 2017). These epipelic diatoms are known to photo-regulate using both physiological and behavioral photoprotection (Cartaxana et al., 2011; Laviale et al., 2015). The species differences observed between the two treatments were mainly related to the non-migrational nature of *Thalassiosira* cf. *proschkinae*, *Thalassiosira* cf. *pseudonana*, *Thalassiosira* cf. *angulata*, *Odontella aurita*, *Raphoneis amphiceros*, *Coconeis speciosa*, and *Nitzschia lorenziana* which will not be captured by our sampling method (Eaton and Moss, 1966). Nevertheless, the two biofilms were strongly dominated by migratory species: *Navicula meulemansii*, *Navicula spartinetensis*, *Gyrosigma limosum*, *Gyrosigma wansbecki* and *Pleurosigma angulatum* and their biovolumes were strongly dominated by *Gyrosigma limosum*, *Gyrosigma wansbecki* and *Pleurosigma angulatum* that, albeit present only in relatively small numbers, correspond to 18.5, 48.1, 22.6 and 17.3, 51.7, 22.2% of the total biovolume (non-migrational and migrational, respectively).

Physiological Photoprotection

In the non-migrational biofilms cells were artificially constrained to immobility and thus had to rely solely on physiological photoprotection to cope with changing light environment. This immobility was characterized by an increase in ϕII_1 and *α-slope* in the LL condition (**Figures 5**, **6**). A ϕII_1 increase indicates that a higher proportion of absorbed light was being used for photosystem II (PSII) photochemistry implying a concomitant

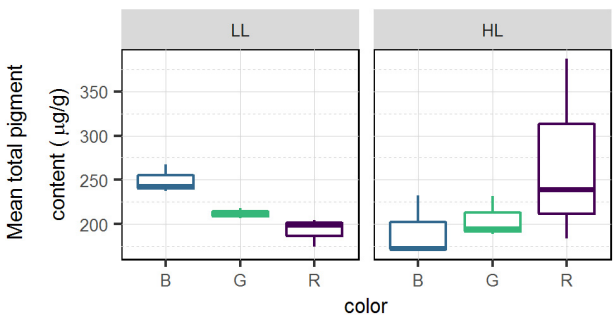

FIGURE 7 | Average total pigment content ($\mu g.g^{-1}$) for each light color and intensity in migrational biofilm (n = 3). Pigments were sampled on the top 2 mm of the sediment using contact cores.

decrease in NPQ from the start of the experiment. This is coherent with the α-slope increase observed in the LL non-migrational biofilms (**Figure 6**) as RLC α-slope increases have been shown to be proportional to NPQ reversal (Cruz and Serôdio, 2008). An α-slope increase over time indicates that a significant amount of NPQ had accumulated overnight in all conditions and was being dissipated over the course of the experiment in the LL conditions. Diatom dark NPQ induction has been previously observed and attributed to a transthylakoidal pH-gradient dependent activation of the XC cycle, due to chlororespiration or to the reverse operation of ATP synthase (Ting and Owens, 1993; Jakob et al., 1999; Dijkman and Kroon,

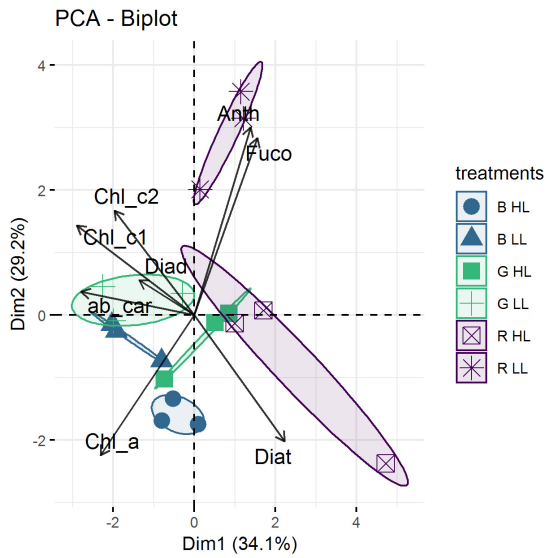

FIGURE 8 | Representation of Principal component analysis (PCA) calculated with pigment percentages from $\mu g.g^{-1}$. The first two PCA dimensions accounted for 29.3 and 26.2%, respectively, of the total variance. Replicates of the same treatment (n = 3) are grouped by confidence interval ellipses (0.95).

2002; Mouget et al., 2004). The decrease of NPQ and the consequent increase of both α-slope and ϕII_1 under LL could be explained by the gradual dissipation of the transthylakoidal proton gradient under low fluence rates (Consalvey et al., 2004a; Serôdio et al., 2005). This NPQ dissipation attests that the LL intensity condition was indeed perceived, for each color, as a non-stressful factor and did not require the development of photoprotective mechanisms hence a gradually increasing *rETRm* (**Table 1**).Within the LL treatments there was no significant differences between NPQ dissipation despite varying Qphar values (**Figure 3**, non-migrational) indicating that below 200 μmol.photons.m^{-2}.s^{-1} of Qphar, NPQ build up was not modulated by the amount of light absorbed. This was further exemplified by the absence of noteworthy differences in EPS that were characterized by the same amount of carbohydrates (**Figure 9**) and proteins. Under HL exposure in non-migrational biofilms photosynthetic parameters ϕII_1 and α-slope showed less NPQ induction under red light (**Figure 6**) with no significant differences between red and dark treatments. Comparatively, green and especially blue light induced much more NPQ build-up in non-migrational HL samples (**Figure 6**). CC concentrations were also significantly higher in HL than LL. These changes in CC production/secretion could reflect a need to readjust the carbohydrate:protein ratio within the cell as an "overflow metabolism" that helps coping with the stressful environmental conditions imposed by exposure to high light intensities (Staats et al., 2000; Orvain et al., 2003; Underwood et al., 2004; Takahashi et al., 2009). At HL there was a strong inverse correlation of $r = -0.92$ ($p < 0.001$) between α-slope and Qphar (**Figure 3**). The same correlation was not observed between CC and Qphar as CC content were not significantly different in HL (**Figure 9**). The physiological role of CC in photoprotection therefore seemed limited to whether or not NPQ was induced but not proportional to the amount of NPQ induction. There was a threshold between 200 and 250 μmol.photons.m^{-2}.s^{-1} of Qphar where light started inducing physiological photoprotection. Despite not having pigment data for the non-migrational biofilms, α-slope and ϕII_1 values observed in HL non-migrational biofilms suggested that blue light, notably due to its higher Qphar value would have had a higher effect in inducing the xantophyll cycle as observed by the strong decrease in α-slope (**Figure 6**) and rETRm (**Table 1**), in comparison to the other two light colors. Previous observations, using similar Qphar intensities (Schellenberger Costa et al., 2013a) or using wavelength dependent absorption cross-section of PSII (PSII effective quanta.s^{-1}) (Schreiber et al., 2012), have shown that despite these standardization growing diatoms in blue light induced significant higher NPQ and *ETRm* values compared to red light (Schreiber et al., 2012; Schellenberger Costa et al., 2013a,b; Jungandreas et al., 2014). Diatoms possess a number of photoreceptors, including blue light sensing aureochrome and red/far-red light sensing phytochrome, hypothesized to mediate photoprotective

TABLE 3 | Main pigment concentration in ug.g^{-1} for migrational biofilm.

	Blue		Green		Red	
μmol.photons.m^{-2}.s^{-1}	**800**	**210**	**800**	**210**	**800**	**210**
Chl *a*	78.58 ± 14.8	102.85 ± 6.72	81.27 ± 8.79	85.99 ± 3.4	106.81 ± 42.6	74.98 ± 6.34
Fuco	69.38 ± 13.03	93.74 ± 6.13	75.98 ± 9.7	77.47 ± 1.96	101.11 ± 39.71	74.28 ± 6.76
Chl *c1*	6.96 ± 1.53	9.87 ± 0.84	7.9 ± 0.76	8.35 ± 0.5	9.41 ± 3	7.35 ± 0.79
Chl *c2*	3.76 ± 0.7	4.72 ± 0.51	3.97 ± 0.49	4.2 ± 0.34	4.84 ± 1.43	3.79 ± 0.37
Chl *b*	2.62 ± 0.82	2.51 ± 0.08	1.7 ± 0.05	1.77 ± 0.14	2.35 ± 1.15	1.69 ± 0.23
ab car	3.62 ± 0.78	4.97 ± 0.33	3.93 ± 0.38	3.84 ± 0.22	4.43 ± 1.11	3.52 ± 0.26
Anth	1.33 ± 0.15	1.53 ± 0.14	1.56 ± 0.08	1.74 ± 0.03	2.2 ± 0.69	2.37 ± 0.24
Diad	15.83 ± 2.79	21.3 ± 1.32	17.28 ± 2.47	20.32 ± 0.6	22.86 ± 8.46	16.36 ± 1.19
Diat	5.91 ± 1.26	3.81 ± 0.08	7.22 ± 0.53	3.53 ± 0.22	10.4 ± 5.02	3.08 ± 0.18
DES	0.27 ± 0.31	0.15 ± 0.06	0.29 ± 0.18	0.15 ± 0.27	0.31 ± 0.37	0.16 ± 0.13

Pigments were sampled on the top 2 mm of the sediment using contact cores. n = 3. ± : standard deviations.

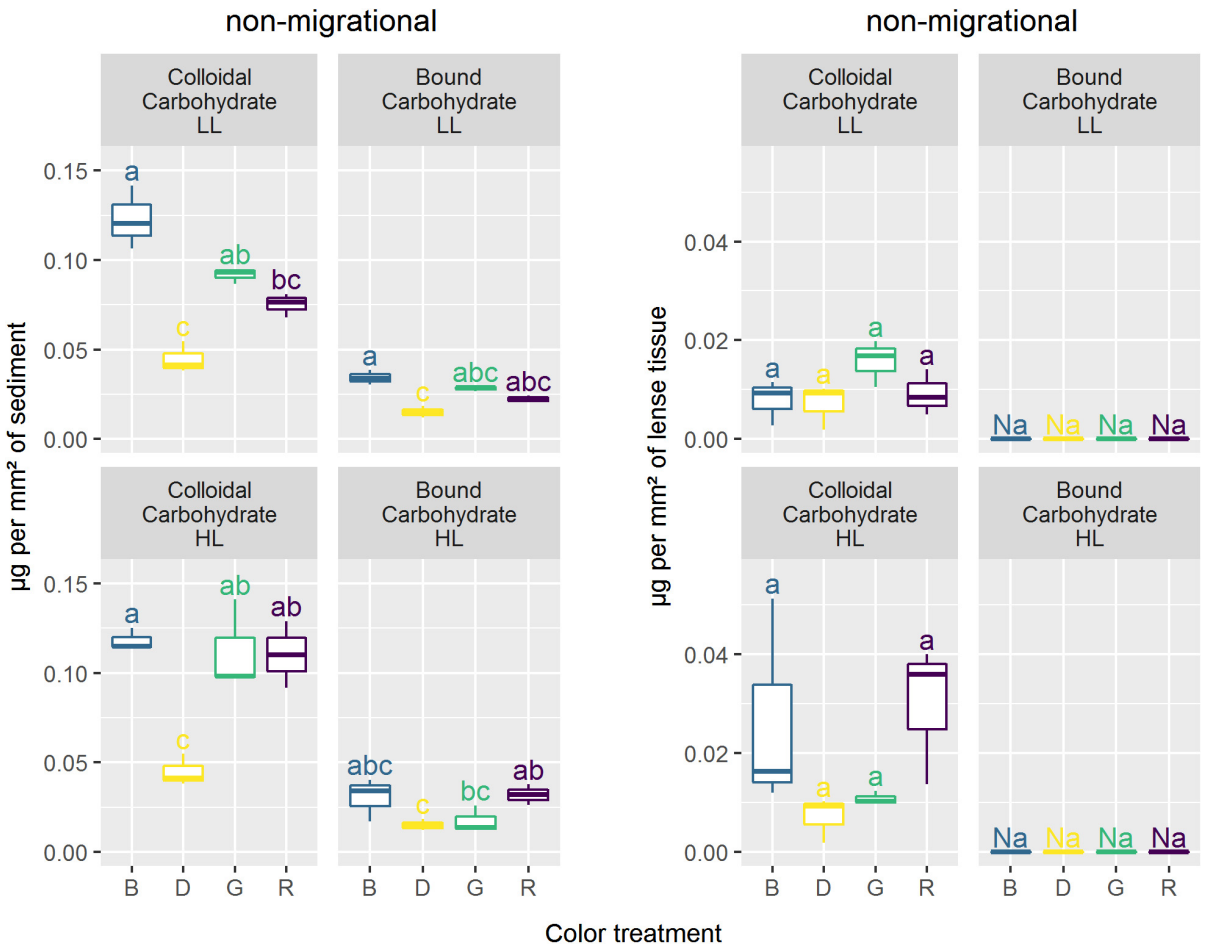

FIGURE 9 | Carbohydrates concentration ($\mu g.mm^{-2}$) in coloidal and bound fraction for the different lights. Similar letters correspond to treatments not significantly different from Tukey multiple comparisons between colors and intensity within each carbohydrate fraction with an alpha of 0.05.

responses (Depauw et al., 2012 and reference therein). The blue photoreceptor Aureochrome 1a was found to repress HL acclimation of *Phaeodactylum tricornutum* in both blue and red light implying a mediated pathway between these lights and aureochrome (Schellenberger Costa et al., 2013b). Similarly, but without correcting for wavelength specific absorption, Brunet et al. (2014) found that *Pseudo-nitzschia multistriata* could not induce HL acclimation with monochromatic wavelengths and required both blue and red light sensing to regulate DES and NPQ production. All aforementioned studies used monospecific culture grown under very different light regime favoring long term acclimation. To our knowledge the effect of light quality on physiological photoprotection has not been investigated on scales of minutes to hours making comparison between studies extremely challenging. Besides, specific absorption and Qphar measurements are highly variable, species specific and susceptible to changes due to DES variation (Fujiki and Taguchi, 2001), cell volume (Fujiki and Taguchi, 2001), "pigment package" effect (Bidigare et al., 1990) and *in vivo* bathochromic shifts (Bidigare et al., 1990). Ideally Qphar should be monitored continuously but is not the only chromatic effect of light and may sometime prove to be unadapted to quantitatively measure light. For instance, frustule nanostructure may change upon exposure to different monochromatic wavelengths (Su et al., 2015) consequently modifying photonic properties either in increasing blue light absorption by the frustule (Yamanaka et al., 2008) or in increasing blue light scalar irradiance thus enhancing the effective intensity of blue light (Goessling et al., 2018). Such effect would not be integrated in Qphar calculation. Consequently, it is uncertain whether different physiological responses at different color wavelengths were only a reflection of different Qphar values or if other chromatics differences would exist.

Biofilm Movement

Light quality effects on migration were strongly dependent on light intensity, with certain wavelengths inducing variable migration responses. Namely, blue and red colors induced intense upward migration movements in LL and HL, respectively. A stronger migration response and diatom accumulation in blue light has been supported by Nultsch (1971) early work on *Nitzschia communis* as well as McLachlan et al. (2009) on *Navicula perminuta* where wavelengths up to 540 µm induced

positive phototropism while red wavelengths did not. Similarly, Wenderoth and Rhiel (2004) observed cell accumulations 1.8 times higher in blue compared to white light (low fluence rate 5 μmol.photons.m^{-2}.s^{-1}). The cited studies were done at low light levels and are consistent with the absorptivity increases we observed in blue LL in comparison to green, red and dark (**Figure 4**), supporting the hypothesis that at low fluence rates blue wavelengths are more efficient at stimulating diatom movements. In diatoms, several light sensors have been evidenced and hypothesized to be involved in the light quality responsive changes in motility (McLachlan et al., 2009; Cohn et al., 2015). Changes in light intensities have been shown to be most sensitive in modulating the whole cell movement near the distal ends of the raphes (Cohn et al., 1999, 2015) and a putative photo-detection system could involve an aureochrome. However, biochemical and functional characterization of these photoreceptors and their chromophores is still very limited (Depauw et al., 2012; Wilhelm et al., 2014). The existence of different species specific motile responses to light quality (Cohn et al., 2015) as well as the lack of current identified receptors at the tips of the cells hinder further conclusions on the role of these photoreceptors. The high correlation, observed in LL, between absorptivity and Qphar (r = 0.74, p < 0.001) suggests that the different migrational responses were a response to the amount of Qphar rather than selective effect of different wavelength and their specific interaction with photoreceptors. Changes observed in absorptivity (**Figure 4**) were paralleled by mean total pigment content (**Figure 7**) for different intensity and treatments. Although this correlation (r = 0.75) was not statistically significant (p = 0.09) it could indicate that the absorptivity parameter, which was measured at the sediment surface, was linked to the biomass (pigments) measured in the 2 mm deep contact core. This strong correlation could imply that cells would have migrated deeper than 2 mm in the lower absorptivity samples. Diatom speeds have not been often measured in natural sediments but the few available datasets supports the possibility that diatoms could have migrated more than 2 mm during the course of the experiment (4.5 h). Namely, using values presented by Hay et al. (1993) the biofilm would have been able to move at least 2.7 mm in the 4.5 h. The downward migration in blue HL could be related to a light-stress response due to higher Qphar values resulting in less accumulation of cells at the sediment surface. This light stress would be accompanied by an increase in NPQ build-up, which would induce a photoprotective downward response or a reduced upward migration in blue light from the start of the experiment. This would be consistent with previous observations that have described light thresholds between 500 and 1000 μmol.photons.m^{-2}.s^{-1} for inducing an avoidance response for both blue (450 nm) and green (550 nm) lights (Cohn, 2001). Furthermore, there is a general consensus that diatom photoaccumulation and photodispersal are intensity dependent whereby low to moderate white light stimulate upward migration and high light promotes downward migration (Serôdio et al., 2008; Du et al., 2010, 2018; Perkins et al., 2010; Coelho et al., 2011; Laviale et al., 2016). The absorptivity changes followed a typical biphasic dose response to Qphar shifting from a positive phototaxis at a theoric maximum between 200 and 250 μmol.photons.m^{-2}.s^{-1} to a negative or downregulated positive phototaxis. Our hypothesis is that above 250 μmol.photons.m^{-2}.s^{-1} of Qphar the onset and amount of NPQ – proportional to Qphar – (**Figure 3**) downregulated behavioral positive phototaxis. However, the light intensity thresholds and the spectral limits described in previous works are very variable and it is possible that the recorded differences are partially the result of the complexity of measuring light environments inside the sediment. Many factors will affect the light received by a diatom incorporated in microphytobenthic biofilms, e.g., organic matter, type of sediment particles, biofilm density, species composition, water content, etc. All these factors will produce different absorption and scattering effects that will affect the intensity and light spectral quality (e.g., Kühl et al., 1994). Nonetheless, regardless of light color, absorptivity increased significantly with time in both LL and HL treatments in comparison to dark controls, which suggests that light intensities were never high enough to completely inhibit upward migration in our conditions. Benthic diatoms are capable of positioning themselves in a light gradient at sediment depths where light exposure is optimal. This optimal depth may vary with photoacclimation status and light intensity tolerance tresholds that induce photoinhibition (Ezequiel et al., 2015) and our data supports the hypothesis that diatom optimal depth will vary as an interaction between light intensity and light quality to adjust to the optimal Qphar light.

Behavioral and Physiological Interplay

The LL migrational biofilms showed a similar trend of increasing ϕII_1 as the LL non-migrational biofilms albeit with less intensity (**Figure 5**). The smaller ϕII_1 increase in migrational biofilms is likely due to an already higher absolute ϕII_1 value at the onset of the experiment. $\phi II_1$and α-slope in LL migrational biofilms increased significantly more under red light, perhaps as a positive tradeoff for having produced little CC (**Figure 9**) and migrated less than other colors (**Figure 4**). In LL intensities there was significant carbohydrate production in blue and green light which was not seen in the non-migrational biofilm. Colloidal carbohydrate concentration (**Figure 9**), mean total pigment (**Figure 7**) and absorptivity (**Figure 4**) followed the same pattern, being highest in blue and lowest in red. These similar patterns could be the result of polysaccharide secretion produced by diatoms during their vertical movements (Pniewski et al., 2015). At these non-stressful LL intensities photo-regulation was mainly dominated by behavioral positive phototaxi to increase light exposure as a response to increasing Qphar values. Exposing migrational biofilms to HL induced a decrease in α-slope and ϕII, which implied physiological photoprotection due to stress exerted by the light intensities. Analysis of the relative pigment percentage showed significant differences (**Figure 8**). HL samples were characterized by a significant higher Diat relative concentration and a lower relative concentration of Diad which is consistent with the xanthophyll cycle operation (Olaizola and Yamamoto, 1994; Lavaud et al., 2004). Colorwise there were no significant DES differences between color treatments (**Table 3**) despite very different Qphar amount. Similarly, at

HL in migrational biofilms, despite a differential migration between colors there were no significant differences in either α-slope (**Figure 3**) or EPS secretion for different colors. This implies that, even if blue light has the potential to induce an higher NPQ and DES (see physiological photoprotection discussion), diatoms can migrate to different sediment depths. Diatoms seemed to position themselves at an optimal depth as a response to the interaction between light intensity and spectral composition. At these depths they might maximize their CC production for both behavioral and physiological photoprotection, thus showing no obvious differences in CC concentration between the different colors (**Figure 9**). These result contrasts with previous observations (Perkins et al., 2001) that did not find significant colloidal carbohydrates accumulation differences at the end of the migration between shaded and unshaded biofilms. It is noteworthy to stress that samples from natural sediments will contain EPS from a range of sources (bacteria, detritus, and dissolved organic matter) (Smith and Underwood, 1998) and while our extraction technique has been proposed as a standardized method for microphytobenthos (Takahashi et al., 2009) other extraction techniques may have had different EPS fractions making comparison with previous studies difficult (Underwood et al., 1995, 2004; Smith and Underwood, 2000; De Brouwer and Stal, 2002). It is possible that blue and red photoreceptors are involved in tailoring the specific behavioral photoprotective responses. In natural conditions blue/red ratio is a very informative cue for diatoms, changing during tides, twilight and with depth (Ragni and D'Alcalà, 2004; Spitschan et al., 2016). However the exact pathway and signal cascading remain to be elucidated. We hypothesize that the trigger for the vertical migration movements and behavioral photoprotection is linked to an NPQ mechanism or some other light-stress induced mechanism, e.g., ROS production. This would be in agreement with other observations of diatoms using motility to select their optimal light exposure based on their photophysiological status (Ezequiel et al., 2015; Cartaxana et al., 2016) emphasizing the behavioral role of migration in regulating photosynthesis. Nevertheless, while migration compensated the different NPQ and DES levels observed in non-migrational biofilm between the different color treatments we still observed higher *rETRm* values in blue light migrational biofilms (**Table 2**). These differences show that despite an active behavioral photoprotection mechanism, light specific wavelengths affected photosynthesis differently. Further investigation on the role of photoreceptors, wavelength specific chloroplast aggregation (Furukawa et al., 1998; Noyes et al., 2008) or frustule waveguiding properties (Shihira-Ishikawa et al., 2007) could shed some light on the underlying mechanisms between these two types of photoprotection.

CONCLUSION

Overall there was a strong interaction between light intensity and spectral quality in inducing diatoms migration and behavioral photoprotection. The difficult task of disentangling the respective role of light inherent properties showcased how relevant considering both light quality and intensity helped understanding the underlying mechanisms of biofilm photoprotection. While not accounting for all chromatic effects of light, the use of Qphar proved to finely integrate and correctly correlate to the light quality and intensity interactions. The higher impact of blue light in stimulating ETR and NPQ development in comparison to red remains to be elucidated but was largely dependent on how much light was being absorbed. These differences are largely reduced in the sediment biofilms due to finely tuned vertical migration movements, supporting the hypothesis of epipelic diatom photoprotection being governed by behavioral mechanisms. Furthermore, it strongly suggests a wavelength and Qphar dependent light stress threshold that triggers NPQ development and consequently override or downregulate upward movements. Our data supports the hypothesis that diatoms accumulation and migration can extend deeper than 2 mm. The absence of light cues at these depths and the fast migration in a matter of few hours could have implication for future experimental design of microphytobenthos migrational studies.

DATA AVAILABILITY STATEMENT

All datasets generated for this study are included in the article/supplementary material.

AUTHOR CONTRIBUTIONS

AP, BJ, PD, and CH: conceptualization. AP, CH, and BJ: formal analysis, visualization, and writing – review and editing. AP and BJ: investigation and writing – original draft. BJ and CH: methodology and validation.

FUNDING

This research was supported under the BIO-Tide project, funded through the 2015–2016 BiodivERsA COFUND call for research proposals, with the national funders BelSPO, FWO, ANR, and SNSF.

REFERENCES

Barnett, A., Méléder, V., Blommaert, L., Lepetit, B., Gaudin, P., Vyverman, W., et al. (2015). Growth form defines physiological photoprotective capacity in intertidal benthic diatoms. *ISME J.* 9, 32–45. doi: 10.1038/ismej.2014.105

Bidigare, R. R., Ondrusek, M., Fisheries, S., and Kiefer, D. A. (1990). "In-vivo absorption properties of algal pigments," in *Proceedings of the 1990 Technical Symposium on Optics, Electro-Optics, and Sensors*, Orlando, FL, 290–301. doi: 10.1117/12.21451

Blommaert, L., Lavaud, J., Vyverman, W., and Sabbe, K. (2018). Behavioural versus physiological photoprotection in epipelic and epipsammic benthic diatoms. *Eur. J. Phycol.* 53, 146–155. doi: 10.1080/09670262.2017.1397197

Brunet, C., Chandrasekaran, R., Barra, L., Giovagnetti, V., Corato, F., and Ruban, A. V. (2014). Spectral radiation dependent photoprotective mechanism in the

diatom Pseudo-nitzschia multistriata. *PLoS One* 9:e87015. doi: 10.1371/journal.pone.0087015

Cartaxana, P., Cruz, S., Gameiro, C., and Kühl, M. (2016). Regulation of intertidal microphytobenthos photosynthesis over a diel emersion period is strongly affected by diatom migration patterns. *Front. Microbiol.* 7:872. doi: 10.3389/fmicb.2016.00872

Cartaxana, P., Ruivo, M., Hubas, C., Davidson, I., Serôdio, J., and Jesus, B. (2011). Physiological versus behavioral photoprotection in intertidal epipelic and epipsammic benthic diatom communities. *J. Exp. Mar. Biol. Ecol.* 405, 120–127. doi: 10.1016/j.jembe.2011.05.027

Cartaxana, P., and Serôdio, J. (2008). Inhibiting diatom motility: A new tool for the study of the photophysiology of intertidal microphytobenthic biofilms. *Limnol. Oceanogr. Methods* 6, 466–476. doi: 10.4319/lom.2008.6.466

Chevalier, E., Gévaert, F., and Créach, A. (2010). In situ photosynthetic activity and xanthophylls cycle development of undisturbed microphytobenthos in an intertidal mudflat. *J. Exp. Mar. Biol. Ecol.* 385, 44–49. doi: 10.1016/j.jembe.2010.02.002

Clementson, L. A., and Wojtasiewicz, B. (2019). Dataset on the absorption characteristics of extracted phytoplankton pigments. *Data Brief* 24:103875. doi: 10.1016/j.dib.2019.103875

Coelho, H., Vieira, S., and Serôdio, J. (2011). Endogenous versus environmental control of vertical migration by intertidal benthic microalgae. *Eur. J. Phycol.* 46, 271–281. doi: 10.1080/09670262.2011.598242

Cohn, S. A. (2001). Chapter 13 Photo-stimulated effects on diatom motility. *Compr. Ser. Photosci.* 1, 375–401. doi: 10.1016/S1568-461X(01)80017-X

Cohn, S. A., Halpin, D., Hawley, N., Ismail, A., Kaplan, Z., Kordes, T., et al. (2015). Comparative analysis of light-stimulated motility responses in three diatom species. *Diatom Res.* 30, 213–225. doi: 10.1080/0269249X.2015.1058295

Cohn, S. A., Spurck, T. P., and Pickett-Heaps, J. D. (1999). High energy irradiation at the leading tip of moving diatoms causes a rapid change of cell direction. *Diatom Res.* 14, 193–206. doi: 10.1080/0269249X.1999.9705466

Consalvey, M. (2002). *The Structure and Function of Microphytobenthic Biofilms*. Available online at: https://hdl.handle.net/10023/2682 (accessed February 03, 2020).

Consalvey, M., Jesus, B., Perkins, R. G., Brotas, V., Underwood, G. J., and Paterson, D. M. (2004a). Monitoring migration and measuring biomass in benthic biofilms: the effects of dark/far-red adaptation and vertical migration on fluorescence measurements. *Photosyn. Res.* 81, 91–101. doi: 10.1023/B:PRES.0000028397.86495.b5

Consalvey, M., Paterson, D. M., and Underwood, G. J. C. (2004b). The ups and down of life in a benthic biofilm: migration of benthic diatoms. *Diatom Res.* 19, 181–202. doi: 10.1080/0269249X.2004.9705870

Cruz, S., and Serôdio, J. (2008). Relationship of rapid light curves of variable fluorescence to photoacclimation and non-photochemical quenching in a benthic diatom. *Aquat. Bot.* 88, 256–264. doi: 10.1016/j.aquabot.2007.11.001

De Brouwer, J. F., and Stal, L. J. (2002). Daily fluctuations of exopolymers in cultures of the benthic diatoms *Cylindrotheca closterium* and *Nitzschia* sp. (Bacillariophyceae). *J. Phycol.* 38, 464–472. doi: 10.1046/j.1529-8817.2002.01164.x

Depauw, F. A., Rogato, A., D'Alcalá, M. R., and Falciatore, A. (2012). Exploring the molecular basis of responses to light in marine diatoms. *J. Exp. Bot.* 63, 1575–1591. doi: 10.1093/jxb/ers005

Dijkman, N. A., and Kroon, B. M. A. (2002). Indications for chlororespiration in relation to light regime in the marine diatom *Thalassiosira weissflogii*. *J. Photochem. Photobiol. B Biol.* 66, 179–187.

Du, G., Yan, H., Liu, C., and Mao, Y. (2018). Behavioral and physiological photoresponses to light intensity by intertidal microphytobenthos. *J. Oceanol. Limnol.* 36, 293–304.

Du, G. Y., Oak, J.-H. H., Li, H., and Chung, I.-K. K. (2010). Effect of light and sediment grain size on the vertical migration of benthic diatoms. *Algae* 25, 133–140. doi: 10.4490/algae.2010.25.3.133

DuBois, M., Gilles, K. A., Hamilton, J. K., Rebers, P. A., and Smith, F. (1956). Colorimetric method for determination of sugars and related substances. *Anal. Chem.* 28, 350–356. doi: 10.1021/ac60111a017

Eaton, J. W., and Moss, B. (1966). The estimation of numbers and pigment content in epipelic algal populations. *Limnol. Oceanogr.* 11, 584–595. doi: 10.4319/lo.1966.11.4.0584

Eilers, P. H. C., and Peeters, J. C. H. (1988). A model for the relationship between light intensity and the rate of photosynthesis in phytoplankton. *Ecol. Model.* 42, 199–215. doi: 10.1111/jpy.12060

Ezequiel, J., Laviale, M., Frankenbach, S., Cartaxana, P., and Serôdio, J. (2015). Photoacclimation state determines the photobehaviour of motile microalgae: the case of a benthic diatom. *J. Exp. Mar. Biol. Ecol.* 468, 11–20. doi: 10.1016/j.jembe.2015.03.004

Frankenbach, S., Pais, C., Martinez, M., Laviale, M., Ezequiel, J., and Serôdio, J. (2014). Evidence for gravitactic behaviour in benthic diatoms. *Eur. J. Phycol.* 49, 429–435. doi: 10.1080/09670262.2014.974218

Frølund, B., Palmgren, R., Keiding, K., and Nielsen, P. H. (1996). Extraction of extracellular polymers from activated sludge using a cation exchange resin. *Water Res.* 30, 1749–1758.

Fujiki, T., and Taguchi, S. (2001). Relationship between light absorption and the xanthophyll-cycle pigments in marine diatoms. *Plankton Biol. Ecol.* 48, 96–103.

Furukawa, T., Watanabe, M., and Shihira-Ishikawa, I. (1998). Green- and blue-light-mediated chloroplast migration in the centric diatom *Pleurosira laevis*. *Protoplasma* 203, 214–220. doi: 10.1007/BF01279479

Gilbert, M., Domin, A., Becker, A., and Wilhelm, C. (2000). Estimation of primary productivity by chlorophyll a *in vivo* fluorescence in freshwater phytoplankton. *Photosynthetica* 38, 111–126. doi: 10.1023/A:1026708327185

Goessling, J. W., Frankenbach, S., Ribeiro, L., Serôdio, J., and Kühl, M. (2018). Modulation of the light field related to valve optical properties of raphid diatoms: implications for niche differentiation in the microphytobenthos. *Mar. Ecol. Prog. Ser.* 588, 29–42. doi: 10.3354/meps12456

Häder, D.-P. (1986). Signal perception and amplification in photomovement of prokaryotes. *Biochim. Biophys. Acta* 864, 107–122.

Hay, S. I., Maitland, T. C., and Paterson, D. M. (1993). The speed of diatom migration through natural and artificial substrata. *Diatom Res.* 8, 371–384. doi: 10.1080/0269249x.1993.9705268

Haynes, K., Hofmann, T. A., Smith, C. J., Ball, A. S., Underwood, G. J. C., and Osborn, A. M. (2007). Diatom-derived carbohydrates as factors affecting bacterial community composition in estuarine sediments. *Appl. Environ. Microbiol.* 73, 6112–6124.

Hernández Fariñas, T., Ribeiro, L., Soudant, D., Belin, C., Bacher, C., Lampert, L., et al. (2017). Contribution of benthic microalgae to the temporal variation in phytoplankton assemblages in a macrotidal system. *J. Phycol.* 53, 1020–1034. doi: 10.1111/jpy.12564

Heukelem, L. V., and Thomas, C. S. (2001). Computer-assisted high-performance liquid chromatography method development with applications to the isolation and analysis of phytoplankton pigments. *J. Chromatogr. A* 910, 31–49.

Hillebrand, H., Dürselen, C.-D., Kirschtel, D., Pollingher, U., and Zohary, T. (1999). Biovolume calculation for pelagic and benthic microalgae. *J. Phycol.* 35, 403–424. doi: 10.1046/j.1529-8817.1999.3520403.x

Jakob, T., Goss, R., and Wilhelm, C. (1999). Activation of diadinoxanthin de-epoxidase due to a chlororespiratory proton gradient in the dark in the diatom *Phaeodactylum tricornutum*. *Plant Biol.* 1, 76–82. doi: 10.1111/j.1438-8677.1999.tb00711.x

Jauffrais, T., Drouet, S., Turpin, V., Méléder, V., Jesus, B., Cognie, B., et al. (2015). Growth and biochemical composition of a microphytobenthic diatom (*Entomoneis paludosa*) exposed to shorebird (*Calidris alpina*) droppings. *J. Exp. Mar. Biol. Ecol.* 469, 83–92. doi: 10.1016/j.jembe.2015.04.014

Jesus, B., Brotas, V., Ribeiro, L., Mendes, C. R., Cartaxana, P., and Paterson, D. M. (2009). Adaptations of microphytobenthos assemblages to sediment type and tidal position. *Cont. Shelf Res.* 29, 1624–1634. doi: 10.1016/j.csr.2009.05.006

Jesus, B., Perkins, R. G., Consalvey, M., Brotas, V., and Paterson, D. M. (2006). Effects of vertical migrations by benthic microalgae on fluorescence measurements of photophysiology. *Mar. Ecol. Prog. Ser.* 315, 55–66. doi: 10.3354/meps315055

Jungandreas, A., Costa, B. S., Jakob, T., Von Bergen, M., Baumann, S., and Wilhelm, C. (2014). The acclimation of *Phaeodactylum tricornutum* to blue and red light does not influence the photosynthetic light reaction but strongly disturbs the carbon allocation pattern. *PLoS One* 9:e99727. doi: 10.1371/journal.pone.0099727

Kühl, M., Lassen, C., and Jorgensen, B. B. (1994). Light penetration and light intensity in sandy marine sediments measured with irradiance and scalar irradiance fiber-optic microprobes. *Mar. Ecol. Prog. Ser.* 105, 139–148. doi: 10.3354/meps105139

Kume, A. (2018). Importance of the green color, absorption gradient, and spectral absorption of chloroplasts for the radiative energy balance of leaves. *J. Plant Res.* 130, 501–514. doi: 10.1007/s10265-017-0910-z

Lavaud, J., and Goss, R. (2014). "The peculiar features of non-photochemical fluorescence quenching in diatoms and brown algae," in *Non-Photochemical Quenching and Energy Dissipation in Plants, Algae and Cyanobacteria*, eds B. Demmig-Adams, G. Garab, W. Adams III, and Govindjee (Dordrecht: Springer), 421–443. doi: 10.1007/978-94-017-9032-1_20

Lavaud, J., Rousseau, B., and Etienne, A. L. (2004). General features of photoprotection by energy dissipation in planktonic diatoms (Bacillariophyceae). *J. Phycol.* 40, 130–137. doi: 10.1046/j.1529-8817.2004.03026.x

Laviale, M., Barnett, A., Ezequiel, J., Lepetit, B., Frankenbach, S., Méléder, V., et al. (2015). Response of intertidal benthic microalgal biofilms to a coupled light-temperature stress: evidence for latitudinal adaptation along the Atlantic coast of Southern Europe. *Environ. Microbiol.* 17, 3662–3677. doi: 10.1111/1462-2920.12728

Laviale, M., Frankenbach, S., and Serôdio, J. (2016). The importance of being fast: comparative kinetics of vertical migration and non-photochemical quenching of benthic diatoms under light stress. *Mar. Biol.* 163:10.

MacIntyre, H. L., Geider, R. J., and Miller, D. C. (1996). Microphytobenthos: the ecological role of the "Secret Garden" of unvegetated, shallow-water marine habitats. I. Distribution, abundance and primary production. *Estuaries* 19, 186–201. doi: 10.2307/1352224

McLachlan, D. H., Brownlee, C., Taylor, A. R., Geider, R. J., and Underwood, G. J. C. (2009). Light-induced motile responses of the estuarine benthic diatoms Navicula perminuta and *Cylindrotheca closterium* (bacillariophyceae). *J. Phycol.* 45, 592–599. doi: 10.1111/j.1529-8817.2009.00681.x

Méléder, V., Rincé, Y., Barillé, L., Gaudin, P., and Rosa, P. (2007). Spatiotemporal changes in microphytobenthos assemblages in a macrotidal flat (Bourgneuf Bay, France). *J. Phycol.* 43, 1177–1190. doi: 10.1111/j.1529-8817.2007.00423.x

Mertens, A., Witkowski, A., Lange-Bertalot, H., Ribeiro, L., and Rhiel, E. (2014). *Navicula meulemansii* sp. nov., (Bacillariophyaceae) from brackish waters in Europe and the U.S.A. Nova Hedwigia 98, 201–212. doi: 10.1127/0029-5035/2013/0152

Mitbavkar, S., and Anil, A. C. (2004). Vertical migratory rhythms of benthic diatoms in a tropical intertidal sand flat: Influence of irradiance and tides. *Mar. Biol.* 145, 9–20.

Mouget, J. L., Rosa, P., and Tremblin, G. (2004). Acclimation of Haslea ostrearia to light of different spectral qualities - Confirmation of 'chromatic adaptation' in diatoms. *J. Photochem. Photobiol. B Biol.* 75, 1–11. doi: 10.1016/j.jphotobiol.2004.04.002

Noyes, J., Sumper, M., and Vukusic, P. (2008). Light manipulation in a marine diatom. *J. Mater. Res.* 23, 3229–3235. doi: 10.1557/jmr.2008.0381

Nultsch, W. (1971). Phototactic and photokinetic action spectra of the diatom Nitschia communis. *Photochem. Photobiol.* 14, 705–712. doi: 10.1111/j.1751-1097.1971.tb06209.x

Olaizola, M., and Yamamoto, H. Y. (1994). Short-term response of the diadinoxanthin cycle and fluorescence yield to high irradiance in Chaetoceros muelleri (Bacillariophyceae). *J. Phycol.* 30, 606–612. doi: 10.1111/j.0022-3646.1994.00606.x

Olenina, I., Hajdu, S., Edler, L., Andersson, A., Wasmund, N., Busch, S., et al. (2006). *Biovolumes and size-classes of phytoplankton in the Baltic Sea HELCOM Balt.Sea Environ. Proc. No. 106*. Available online at: http://helcom.fi/Lists/Publications/BSEP106.pdf (accessed February 03, 2020).

Orvain, F., Galois, R., Barnard, C., Sylvestre, A., Blanchard, G., and Sauriau, P. G. (2003). Carbohydrate production in relation to microphytobenthic biofilm development: an integrated approach in a tidal mesocosm. *Microb. Ecol.* 45, 237–251.

Paterson, D. (1989). Short-term changes in the erodibility of intertidal cohesive sediments related to the migratory behaviour of epipelic diatoms. *Limnol. Oceanogr.* 34, 223–234. doi: 10.4319/lo.1989.34.1.0223

Paterson, D. M. (1986). The migratory behaviour of diatom assemblages in a laboratory tidal scanning electron microscopy micro-ecosystem examined by low temperature. *Diatom Res.* 1, 227–239. doi: 10.1080/0269249X.1986.9704971

Paterson, D. M., Perkins, R., Consalvey, M., and Underwood, G. J. C. (2003). "Ecosystem function, cell micro-cycling and the structure of transient biofilms," in *Fossil and Recent Biofilms*, eds W. E. Krumbein, D. M. Paterson, and G. A. Zavarzin (Dordrecht: Springer), 47–63. doi: 10.1007/978-94-017-0193-8_3

Paulmier, G. (1997). *Atlas des Diatomophycées des Côtes Françaises et des Aires Marines Adjacentes*. Available online at: https://archimer.ifremer.fr/doc/00000/2452/ (accessed February 03, 2020).

Perkins, R., Underwood, G., Brotas, V., Snow, G., Jesus, B., and Ribeiro, L. (2001). Responses of microphytobenthos to light: primary production and carbohydrate allocation over an emersion period. *Mar. Ecol. Prog. Ser.* 223, 101–112. doi: 10.3354/meps223101

Perkins, R. G., Lavaud, J., Serôdio, J., Mouget, J. L., Cartaxana, P., Rosa, P., et al. (2010). Vertical cell movement is a primary response of intertidal benthic biofilms to increasing light dose. *Mar. Ecol. Prog. Ser.* 416, 93–103. doi: 10.3354/meps08787

Pniewski, F. F., Biskup, P., Bubak, I., Richard, P., Latała, A., and Blanchard, G. (2015). Photo-regulation in microphytobenthos from intertidal mudflats and non-tidal coastal shallows. *Estuar. Coast. Shelf Sci.* 152, 153–161. doi: 10.1016/j.ecss.2014.11.022

R Core Team (2017). *R: A Language and Environment for Statistical Computing*. Vienna: R Foundation for Statistical Computing.

Ragni, M., and D'Alcalà, M. R. (2004). Light as an information carrier underwater. *J. Plankton Res.* 26, 433–443. doi: 10.1093/plankt/fbh044

Ribeiro, L. L. (2010). *Intertidal Benthic Diatoms of the Tagus Estuary: Taxonomic Composition and Spatial-Temporal Variation*. Ph.D. dissertation, University of Lisbon, Lisbon.

Round, F. E. (1965). The epipsammon; a relatively unknown freshwater algal association. *Br. Phycol. Bull.* 2, 456–462. doi: 10.1080/00071616500650071

Round, F. E., and Happey, C. M. (1965). Persistent, vertical-migration rhythms in benthic microflora: Part IV a diurnal rhythm of the epipelic diatom association in non-tidal flowing water. *Br. Phycol. Bull.* 2, 463–471. doi: 10.1080/00071616500650081

Schellenberger Costa, B., Jungandreas, A., Jakob, T., Weisheit, W., Mittag, M., and Wilhelm, C. (2013a). Blue light is essential for high light acclimation and photoprotection in the diatom *Phaeodactylum tricornutum*. *J. Exp. Bot.* 64, 483–493. doi: 10.1093/jxb/ers340

Schellenberger Costa, B., Sachse, M., Jungandreas, A., Bartulos, C. R., Gruber, A., Jakob, T., et al. (2013b). Aureochrome 1a is involved in the photoacclimation of the diatom *Phaeodactylum tricornutum*. *PLoS One* 8:e74451 doi: 10.1371/journal.pone.0074451

Schreiber, U., Klughammer, C., and Kolbowski, J. (2012). Assessment of wavelength-dependent parameters of photosynthetic electron transport with a new type of multi-color PAM chlorophyll fluorometer. *Photosyn. Res.* 113, 127–144.

Serôdio, J., Cruz, S., Vieira, S., and Brotas, V. (2005). Non-photochemical quenching of chlorophyll fluorescence and operation of the xanthophyll cycle in estuarine microphytobenthos. *J. Exp. Mar. Biol. Ecol.* 326, 157–169. doi: 10.1016/j.jembe.2005.05.011

Serôdio, J., Da Silva, J. M., and Catarino, F. (1997). Nondestructive tracing of migratory rhythms of intertidal benthic microalgae using in vivo chlorophyll a fluorescence. *J. Phycol.* 33, 542–553. doi: 10.1111/j.0022-3646.1997.00542.x

Serôdio, J., Ezequiel, J., Barnett, A., Mouget, J. L., Meåéder, V., Laviale, M., et al. (2012). Efficiency of photoprotection in microphytobenthos: role of vertical migration and the xanthophyll cycle against photoinhibition. *Aquat. Microb. Ecol.* 67, 161–175. doi: 10.3354/ame01591

Serôdio, J., Vieira, S., and Cruz, S. (2008). Photosynthetic activity, photoprotection and photoinhibition in intertidal microphytobenthos as studied in situ using variable chlorophyll fluorescence. *Cont. Shelf Res.* 28, 1363–1375. doi: 10.1016/j.csr.2008.03.019

Shihira-Ishikawa, I., Nakamura, T., Higashi, S. I., and Watanabe, M. (2007). Distinct responses of chloroplasts to blue and green laser microbeam irradiations in the centric diatom *Pleurosira laevis*. *Photochem. Photobiol.* 83, 1101–1109. doi: 10.1111/j.1751-1097.2007.00167.x

Silsbe, G. M., and Kromkamp, J. C. (2012). Modeling the irradiance dependency of the quantum efficiency of photosynthesis. *Limnol. Oceanogr. Methods* 10, 645–652. doi: 10.4319/lom.2012.10.645

Smith, D. J., and Underwood, G. J. (2000). The production of extracellular carbohydrates by estuarine benthic diatoms: the effects of growth phase and

light and dark treatment. *J. Phycol.* 36, 321–333. doi: 10.1046/j.1529-8817.2000.99148.x

Smith, D. J., and Underwood, G. J. C. (1998). Exopolymer production by intertidal epipelic diatoms. *Limnol. Oceanogr.* 43, 1578–1591. doi: 10.4319/lo.1998.43.7.1578

Spitschan, M., Aguirre, G. K., Brainard, D. H., and Sweeney, A. M. (2016). Variation of outdoor illumination as a function of solar elevation and light pollution. *Sci. Rep.* 6:26756. doi: 10.1038/srep26756

Staats, N., Stal, L. J., and Mur, L. R. (2000). Exopolysaccharide production by the epipelic diatom *Cylindrotheca closterium*: effects of nutrient conditions. *J. Exp. Mar. Biol. Ecol.* 249, 13–27.

Su, Y., Lundholm, N., Friis, S. M., and Ellegaard, M. (2015). Implications for photonic applications of diatom growth and frustule nanostructure changes in response to different light wavelengths. *Nano Res.* 8, 2363–2372.

Takahashi, E., Ledauphin, J., Goux, D., and Orvain, F. (2009). Optimising extraction of extracellular polymeric substances (EPS) from benthic diatoms: comparison of the efficiency of six EPS extraction methods. *Mar. Freshw. Res.* 60, 1201–1210. doi: 10.1071/MF08258

Taylor, J. D., McKew, B. A., Kuhl, A., McGenity, T. J., and Underwood, G. J. C. (2013). Microphytobenthic extracellular polymeric substances (EPS) in intertidal sediments fuel both generalist specialist EPS-degrading bacteria. *Limnol. Oceanogr.* 58, 1463–1480. doi: 10.4319/lo.2013.58.4.1463

Ting, C. S., and Owens, T. G. (1993). Photochemical and nonphotochemical fluorescence quenching processes in the diatom *Phaeodactylum tricornutum*. *Plant Physiol.* 101, 1323–1330.

Underwood, G. J., Boulcott, M., Raines, C. A., and Waldron, K. (2004). Environmental effects on exopolymer production by marine benthic diatoms: dynamics, changes in composition, and pathways of production. *J. Phycol.* 40, 293–304. doi: 10.1111/j.1529-8817.2004.03076.x

Underwood, G. J., and Kromkamp, J. (1999). Primary production by phytoplankton and microphytobenthos in estuaries. *Adv. Ecol. Res.* 29, 93–153.

Underwood, G. J. C., Paterson, D. M., and Parkes, R. J. (1995). The measurement of microbial carbohydrate exopolymers from intertidal sediments. *Limnol. Oceanogr.* 40, 1243–1253. doi: 10.4319/lo.1995.40.7.1243

Underwood, G. J. C., Perkins, R. G., Consalvey, M. C., Hanlon, A. R. M., Oxborough, K., Baker, N. R., et al. (2005). Patterns in microphytobenthic primary productivity : species-specific variation in migratory rhythms and photosynthetic efficiency in mixed-species biofilms. *Limnol. Oceanogr.* 50, 755–767. doi: 10.4319/lo.2005.50.3.0755

Walpersdorf, E., Kühl, M., Elberling, B., Andersen, T., Hansen, B., Pejrup, M., et al. (2017). In situ oxygen dynamics and carbon turnover in an intertidal sediment (Skallingen, Denmark). *Mar. Ecol. Prog. Ser.* 566, 49–65. doi: 10.3354/meps12016

Wenderoth, K., and Rhiel, E. (2004). Influence of light quality and gassing on the vertical migration of diatoms inhabiting the Wadden Sea. *Helgoland Mar. Res.* 58, 211–215.

Wilhelm, C., Jungandreas, A., Jakob, T., and Goss, R. (2014). Light acclimation in diatoms: from phenomenology to mechanisms. *Mar. Genomics* 16, 5–15. doi: 10.1016/j.margen.2013.12.003

Yallop, M. L., Winder, B. de, Paterson, D. M., and Stal, L. J. (1994). Comparative structure, primary production and biogenic stabilization of cohesive and non-cohesive marine sediments inhabited by microphytobenthos. *Estuar. Coast. Shelf Sci.* 39, 565–582.

Yamanaka, S., Yano, R., Usami, H., Hayashida, N., Ohguchi, M., Takeda, H., et al. (2008). Optical properties of diatom silica frustule with special reference to blue light. *J. Appl. Phys.* 103:074701. doi: 10.1063/1.2903342

Conflict of Interest: The authors declare that the research was conducted in the absence of any commercial or financial relationships that could be construed as a potential conflict of interest.

Copyright © 2020 Prins, Deleris, Hubas and Jesus. This is an open-access article distributed under the terms of the Creative Commons Attribution License (CC BY). The use, distribution or reproduction in other forums is permitted, provided the original author(s) and the copyright owner(s) are credited and that the original publication in this journal is cited, in accordance with accepted academic practice. No use, distribution or reproduction is permitted which does not comply with these terms.